

## Vectorial Electron Transfer in Donor–Photosensitizer–Acceptor Triads Based on Novel Bis-tridentate Ruthenium Polypyridyl Complexes

Rohan J. Kumar,<sup>[a]</sup> Susanne Karlsson,<sup>[a]</sup> Daniel Streich,<sup>[a]</sup> Alice Rolandini Jensen,<sup>[a]</sup> Michael Jäger,<sup>[a]</sup> Hans-Christian Becker,<sup>[a]</sup> Jonas Bergquist,<sup>[b]</sup> Olof Johansson,<sup>\*,[a]</sup> and Leif Hammarström<sup>\*,[a]</sup>

**Abstract:** The first examples of rodlike donor–photosensitizer–acceptor arrays based on bis-2,6-di(quinolin-8-yl)pyridine Ru<sup>II</sup> complexes **1a** and **3a** for photoinduced electron transfer have been synthesized and investigated. The complexes are synthesized in a convergent manner and are isolated as linear, single isomers. Time-resolved absorption spectroscopy reveals long-lived, photoinduced charge-separated states ( $\tau_{\text{CSS}}$  (**1a**) = 140 ns,  $\tau_{\text{CSS}}$  (**3a**) = 200 ns)

formed by stepwise electron transfer. The overall yields of charge separation ( $\geq 50\%$  for complex **1a** and  $\geq 95\%$  for complex **3a**) are unprecedented for bis-tridentate Ru<sup>II</sup> polypyridyl complexes. This is attributed to the long-

lived excited state of the [Ru(dqp)<sub>2</sub>]<sup>2+</sup> complex combined with fast electron transfer from the donor moiety following the initial charge separation. The rodlike arrangement of donor and acceptor gives controlled, vectorial electron transfer, free from the complications of stereoisomeric diversity. Thus, such arrays provide an excellent system for the study of photoinduced electron transfer and, ultimately, the harvesting of solar energy.

**Keywords:** donor–acceptor systems • electron transfer • photochemistry • ruthenium • tridentate ligands

### Introduction

The complexity of all natural systems on earth is dependent on energy provided by photons from the sun.<sup>[1]</sup> The energy of these photons is stored in chemical bonds through the action of photosynthetic organisms.<sup>[2–4]</sup> A key step in photosynthesis is the directional, multi-step electron-transfer process that separates the charges across a membrane and thereby prevents rapid recombination. The precise directionality of electron transfer in this process ensures a large distance between the electron and the hole, and allows for

efficient build-up of redox equivalents at the oxygen-evolving complex for subsequent oxidation of water.

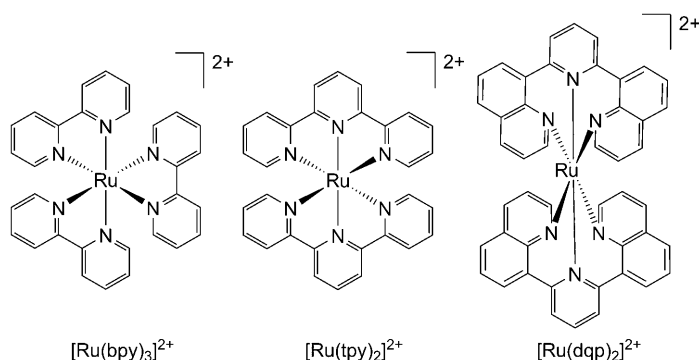
Ruthenium(II) polypyridyl complexes, covalently attached to electron-donor (D) and electron-acceptor (A) units in dyads and triads, have been frequently used as model systems for the charge-separation event in photosynthesis and the study of photoinduced electron transfer.<sup>[5–9]</sup> Also, multinuclear complexes have been proposed as the light-harvesting component in a variety of solar energy generating processes.<sup>[10,11]</sup> The Ru<sup>II</sup> complexes that have been developed for these applications are primarily based on two classes: Ru<sup>II</sup> tris-bipyridine ([Ru(bpy)<sub>3</sub>]<sup>2+</sup>) and Ru<sup>II</sup> bis-terpyridine ([Ru(tpy)<sub>2</sub>]<sup>2+</sup>). Although [Ru(bpy)<sub>3</sub>]<sup>2+</sup> displays ideal photo-physical properties with  $\sim 1\ \mu\text{s}$  metal-to-ligand charge transfer (MLCT) excited-state luminescence lifetimes, the complex is intrinsically chiral (*D*<sub>3</sub> symmetry,  $\Delta$  and  $\Lambda$  configurations), which leads to diastereomeric mixtures in polynuclear assemblies.<sup>[12,13]</sup> Moreover, in donor–photosensitizer–acceptor (D–P–A) charge-separation assemblies, multiple geometrical isomers with different D–A distances are normally obtained.<sup>[14–16]</sup>

Several complications can arise in [Ru(bpy)<sub>3</sub>]<sup>2+</sup>-based D–P–A assemblies because of this heterogeneity. One or several of the isomers may have short charge-separated lifetimes due to the through-space proximity of the donor and accept-

[a] Dr. R. J. Kumar, S. Karlsson, D. Streich, A. Rolandini Jensen, Dr. M. Jäger, Dr. H.-C. Becker, Dr. O. Johansson, Prof. L. Hammarström  
Department of Photochemistry and Molecular Science  
Uppsala University  
Box 523, 751 20 Uppsala (Sweden)  
Fax: (+46) 18-471-6844  
E-mail: leif@fotomol.uu.se  
olof.johansson@fotomol.uu.se

[b] Prof. J. Bergquist  
Department of Physical and Analytical Chemistry  
Uppsala University  
Box 599, 751 24 Uppsala (Sweden)

Supporting information for this article is available on the WWW under <http://dx.doi.org/10.1002/chem.200902716>.



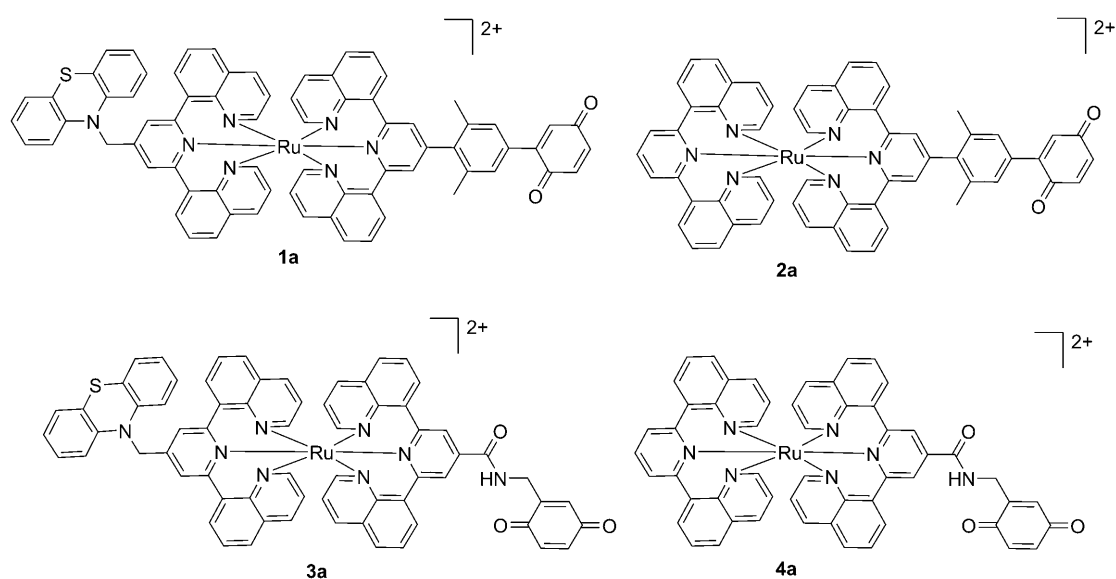
or. Also, the directionality of electron transfer in three-dimensional space will be different in the different isomers, which complicates the coordinated use of electron-transfer products from several triads. Finally, our understanding of D-P-A systems is sometimes complicated by the non-exponential decays arising from the different decay rates of isomeric charge-separated states. Although there are successful routes to the isolation of single isomers of D-P-A assemblies based on the  $[\text{Ru}(\text{bpy})_3]^{2+}$  motif,<sup>[17]</sup> specific formation of only rodlike arrangements of the donor and the acceptor around the photosensitizer would be a more straightforward and less demanding route to vectorial electron transfer.

Conversely,  $[\text{Ru}(\text{tpy})_2]^{2+}$  is achiral ( $D_{2d}$  symmetry) and free of geometrical isomers in D-P-A assemblies when substituted along the  $C_2$  axis. However, the MLCT excited-state lifetime at room temperature is approximately three orders of magnitude shorter than that for  $[\text{Ru}(\text{bpy})_3]^{2+}$ , which leads to inefficient electron-transfer quenching.<sup>[18–20]</sup> The short MLCT excited-state lifetime in  $[\text{Ru}(\text{tpy})_2]^{2+}$  has been attributed to the poor bite angle of the tpy ligands ( $158^\circ$ ), which leads to a weak ligand field, and the complex therefore undergoes rapid non-radiative decay via ligand-field states at

room temperature.<sup>[21]</sup> As an alternative approach the *trans*- $[\text{Ru}(\text{bpy})_2(\text{py})_2]^{2+}$  ( $\text{py}$  = pyridine) motif has been used, but it unfortunately also suffers from a short room-temperature excited-state lifetime and, additionally, poor photostability.<sup>[22]</sup>

Recently, our group has detailed the rational development<sup>[23,24]</sup> and facile synthesis<sup>[25,26]</sup> of a new class of Ru<sup>II</sup> bis-tridentate photosensitizers, based on Ru<sup>II</sup> bis-2,6-di(quinolin-8-yl)pyridine ( $[\text{Ru}(\text{dqp})_2]^{2+}$ ). An almost perfect octahedral coordination sphere, with short and equal Ru–N distances, and consequently a strong ligand field is created through the use of six-membered chelates leading to photophysical properties similar to those of  $[\text{Ru}(\text{bpy})_3]^{2+}$ . The dqp ligands adopt a helical conformation when coordinated to the metal centre and  $[\text{Ru}(\text{dqp})_2]^{2+}$  is best described by the symmetry label  $D_2$  with a  $C_2$  axis running through the pyridyl 4-positions. Therefore,  $[\text{Ru}(\text{dqp})_2]^{2+}$  combines *both* the desirable properties of bis-tridentate complexes (elimination of geometrical isomers) with those of tris-bidentate complexes (favourable photophysical properties).

Herein, we demonstrate for the first time the synthesis and full characterization of D-P-A triads based on  $[\text{Ru}(\text{dqp})_2]^{2+}$  sensitizers (**1a** and **3a**), designed for vectorial photoinduced charge separation. Benzoquinone (Q) and phenothiazine (PTZ) are used as the electron acceptor and electron donor, respectively. The corresponding P–A dyads (**2a** and **4a**) were also prepared as model systems for their corresponding triads. Although there are many examples in which quinones are used as the acceptor in molecular assemblies for photoinduced electron transfer,<sup>[27,28]</sup> the combination of Ru<sup>II</sup> polypyridyl complexes and benzoquinones is not frequently found in the literature.<sup>[29–34]</sup> However, benzoquinones have many attractive properties, such as the high energies of their excited states,<sup>[35]</sup> inaccessible to energy transfer from Ru<sup>II</sup> polypyridyl excited states. Benzoquinones can also be seen as mimics of the plastoquinones in photo-



system II and the purple bacteria reaction centres.<sup>[3]</sup> Additionally, benzoquinones are attractive as they can accept two electrons and two protons, to give the hydroquinone.<sup>[36,37]</sup> This makes them ideal acceptors in systems in which multiple, proton-coupled electron transfer is desired, although this lies beyond the scope of the current study.

## Results and Discussion

**Design and synthesis:** To install the quinone functionality, a 2,5-dimethoxybenzene (DMB) unit was utilized as a masked quinone, to be deprotected and oxidized after coordination to the Ru<sup>II</sup> centre. The DMB precursors **1b–4b** also acted as reference complexes for the corresponding dyads and triads **1a–4a** during electrochemical and photochemical characterization.

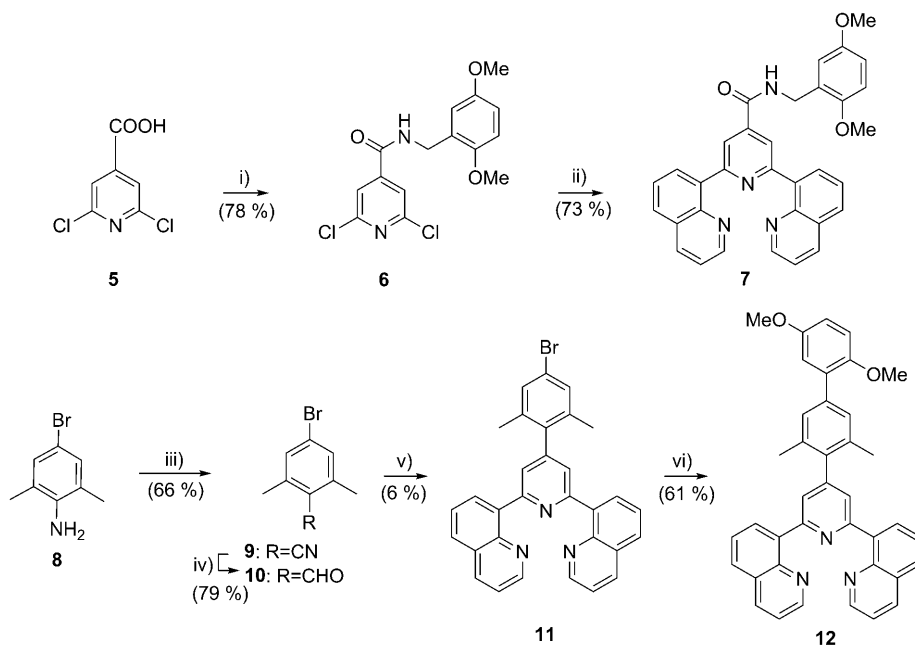
The initial choice for the photosensitizer–acceptor linkage was an amide functionality, governed by the desire to break the conjugation between the photosensitizer and acceptor in order to reduce the electronic coupling between the two systems and decrease the rate of back electron transfer. Our recent electrochemical studies of a variety of dqp-based ruthenium complexes<sup>[24,26]</sup> showed that the substituent at the pyridal 4-position may allow the excited state to be preferentially located on one of the dqp ligands. Thus, it was inferred that the electron-withdrawing amide should also aid the localization of the excited state onto the dqp ligand closest to the acceptor. An *N,N*-dicyclohexylcarbodiimide (DCC)-promoted coupling of dichloroisonicotinic acid (**5**, Scheme 1) with 2,5-dimethoxybenzylamine provided 2,6-dichloro-*N*-(2,5-dimethoxybenzyl)isonicotinamide (**6**), and the quinoline groups were introduced by a Suzuki coupling as described by Jäger et al.<sup>[25]</sup> to give the desired DMB ligand **7**.

Although the amide linkage may have many favourable properties, it also introduced instability to the system, which is discussed in more detail below. Thus, another linkage functionality was explored, a 2,5-dimethylphenyl motif, which is more linear than the amide link. The methyl groups in the 2- and 5-positions serve to force the ring systems of the dqp unit, linker, and acceptor out of plane with one another, which reduces the conjugation of the system and thus the electronic coupling. This system showed greater stability during prepara-

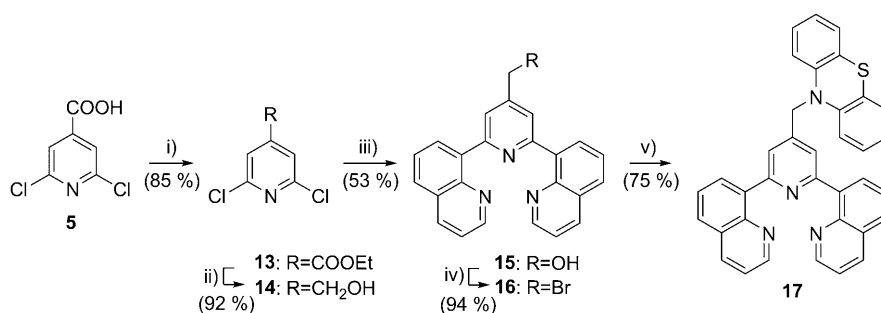
tion and purification than the amide-linked complexes. This linkage was synthesized from 4-bromo-2,6-dimethylaniline (**8**, Scheme 1), from which the corresponding nitrile **9** was obtained under Sandmeyer conditions. Compound **9** was subsequently reduced to the aldehyde **10** by using diisobutylaluminium hydride (DIBAL-H). The dqp motif (**11**) was then introduced through reaction of 8-acetylquinoline and ammonia under basic conditions, in a one-pot reaction as described by Jäger et al.<sup>[25]</sup> The low yield in this step is presumably a result of the additional steric demands placed on the intermediates by the 2,5-dimethyl substitution. However, the enone intermediate was isolated from the reaction mixture in high yield and reacted with further 8-acetylquinoline to give the product. The DMB motif was installed by Suzuki coupling in good yield to give the desired dqp ligand **12**.

For the PTZ linker a methylene group was used, primarily to break conjugation and minimize electronic coupling. The PTZ unit was installed subsequent to the Suzuki coupling to avoid catalyst poisoning by the sulfur atom. Thus, from **5**, esterification followed by NaBH<sub>4</sub> reduction gives the alcohol (**13** and **14**, Scheme 2), which is the substrate for the Suzuki reaction giving **15**. The alcohol was then brominated with PBr<sub>3</sub> (**16**) and the PTZ motif introduced through nucleophilic attack of the deprotonated PTZ (**17**).

With the substituted dqp ligands in hand, synthesis of the desired dyads and triads by complexation to the ruthenium proceeded via tris-acetonitrile intermediates (**18** and **19**, Scheme 3)<sup>[24]</sup> previously reported by our group for this class of ligands.<sup>[26]</sup> The complexation of the second tridentate



Scheme 1. Synthesis of acceptor ligands. Reagents and conditions: i) 2,5-dimethoxybenzylamine, DCC, *N*-hydroxysuccinimide; CH<sub>2</sub>Cl<sub>2</sub>, room temperature, 3 h; ii) 8-quinolinyboronic acid, [Pd(dba)<sub>2</sub>], SPhos, K<sub>2</sub>CO<sub>3</sub>; MeCN, H<sub>2</sub>O, 130 °C, microwave heating, 1 h; iii) NaNO<sub>2</sub>, HCl then NaHCO<sub>3</sub>, KCN, CuCN; H<sub>2</sub>O, 0 to 70 °C, 1 h; iv) DIBAL-H, CH<sub>2</sub>Cl<sub>2</sub>; 0 °C to room temperature, overnight; v) 8-acetylquinoline, KOH, NH<sub>4</sub>OH; 40 °C, 96 h; vi) 2,5-dimethoxyphenylboronic acid, [Pd(dba)<sub>2</sub>], SPhos, K<sub>2</sub>CO<sub>3</sub>; MeCN, H<sub>2</sub>O, 130 °C, microwave heating, 1 h. dba = dibenzylideneacetone, SPhos = 2-dicyclohexylphosphino-2',6'-dimethoxybiphenyl.



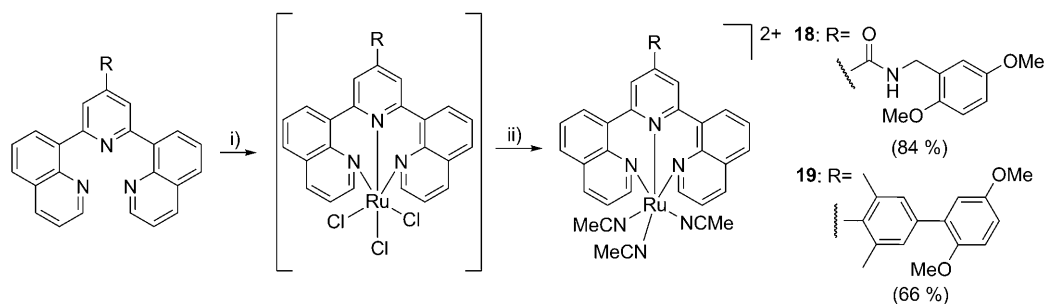
Scheme 2. Synthesis of donor ligand. Reagents and conditions: i)  $\text{H}_2\text{SO}_4$ , EtOH; 80 °C, 2 h; ii)  $\text{NaBH}_4$ ; EtOH, 0 °C to room temperature, 3 h; iii) 8-quinolinyboronic acid,  $[\text{Pd}(\text{dba})_2]$ , SPhos,  $\text{K}_2\text{CO}_3$ ; MeCN,  $\text{H}_2\text{O}$ , 130 °C, microwave heating, 1 h; iv)  $\text{PBr}_3$ ;  $\text{CH}_2\text{Cl}_2$ , 0 °C to room temperature; v)  $\text{NaH}$ , 10H-PTZ; THF, 0 °C to room temperature, overnight.

ligand gave the DMB-containing complexes (**1b–4b**, Scheme 4), which served as reference complexes in the photophysical studies. As discussed before, the use of tris-acetonitrile precursors for the second complexation in *n*BuOH at reflux only gives small amounts of  $\text{Ru}^{\text{II}}$  complexes in which the dqp ligands bind in a facial mode.<sup>[26]</sup> For **1b–4b**, yields were generally good and the products isolated were free of facial isomers, as detected by NMR spectroscopy and LC–MS. Significant care was required in handling many of the complexes; those containing an amide functionality were found to be prone to hydrolysis under aqueous conditions and on standing, even at neutral pH. This decomposition pathway may be responsible for the inability to obtain fitting elemental analysis for **3a**; however, the data are reported for completeness. Additionally, those compounds containing a PTZ motif were oxidized by air to give the sulfoxide on a time frame of minutes to days. The use of conventional Schlenk techniques and dry, degassed solvents was thus employed to prevent decomposition.

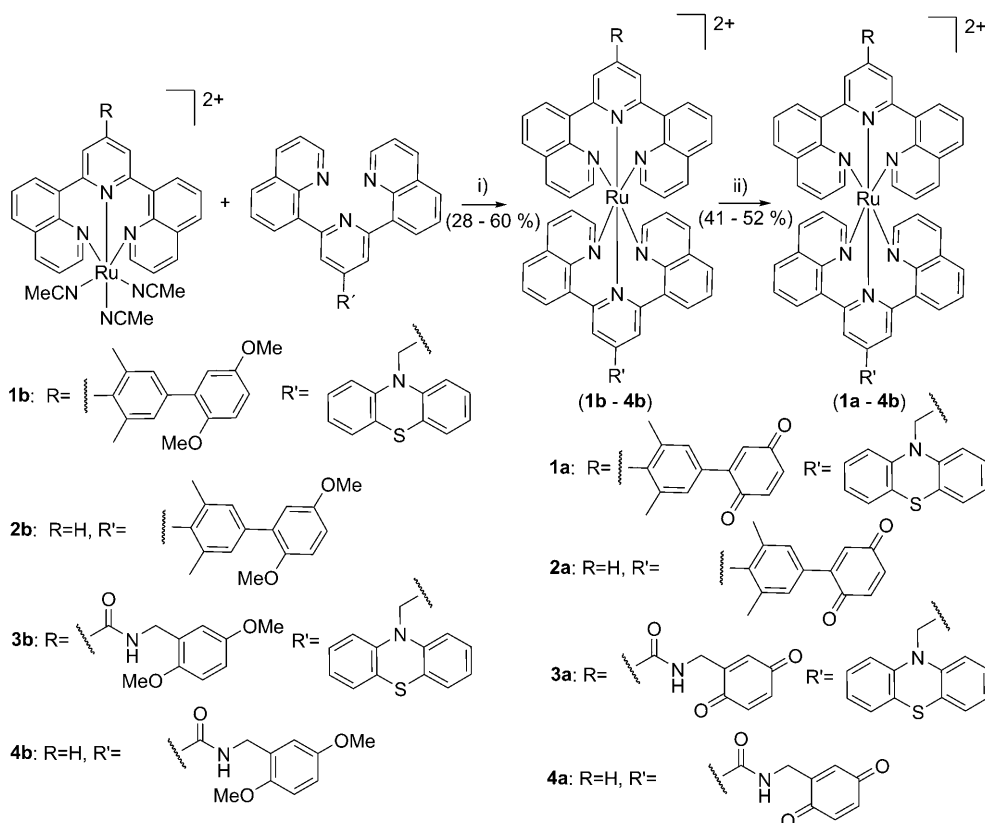
The DMB motif was subsequently deprotected and oxidized to give the target complexes **1a–4a**. For  $[\text{Ru}(\text{bpy})_3]^{2+}$ -based complexes this is routinely achieved in a single step by using ceric ammonium nitrate (CAN). However, the use of this reagent led to decomposition of the complexes, and also for **2b** and **4b** lacking the PTZ unit, which was attributed to the lower oxidation potential of  $[\text{Ru}(\text{dq})_2]^{2+}$  in comparison to  $[\text{Ru}(\text{bpy})_3]^{2+}$ . The use of PbO as reported by Schmidt et al.<sup>[38]</sup> in the synthesis of the extensively studied

porphyrin amide quinone systems<sup>[38,39]</sup> was also excluded given the similar redox potentials of CAN and PbO. Thus, a mild two-step deprotection strategy by using  $\text{BBr}_3$  followed by oxidation with DDQ, as reported by Schanze and Sauer,<sup>[32]</sup> gave the desired quinones in 41–52% yield over the two steps. To ensure purity, the complexes were purified by preparative HPLC as the chloride salt prior to characterization; however, this was not possible with the quinone-containing amide complexes due to the aforementioned hydrolysis of the amide bond. Here, preparative HPLC was undertaken on the DMB complex prior to deprotection and oxidation.

The purification of quinone-containing  $\text{Ru}^{\text{II}}$  polypyridyl complexes free from hydroquinone is a challenge in terms of both isolation and characterization, as has been observed previously.<sup>[29,32,33]</sup> Elemental analysis and HRMS fail to distinguish between the quinone and the hydroquinone. NMR spectroscopy offers a useful tool to discriminate between the two, but can only reliably ensure that the compound is of 95% purity. Examination of the  $^1\text{H}$  proton signals in compounds for which the quinone-containing region of the spectra is not heavily obscured by other signals can indicate purity, and in the case of the amide-linked complexes, one can observe differences in the coupling of the protons alpha to the amide bond depending on the aromatic or non-aromatic nature of the substituent. Figure 1 displays the  $^1\text{H}$  NMR spectra of complexes **4a** and **4b** which show a simple doublet for the  $-\text{CH}_2-\text{NHCO}-$  protons for **4b**, whereas a more complex allylic coupling is observed for **4a** containing the non-aromatic quinone unit; analysis of the spectra indicates a purity of 90–95%. A similar analysis for **3a** indicated up to 30% of the hydroquinone impurity. Attempts to further purify **3a** led to increased amounts of hydroquinone or hydrolysis products. In contrast, for complexes **1a** and **2a** the  $^1\text{H}$  NMR spectra suggest >95% purity. LC–MS analysis of the samples showed a single



Scheme 3. Synthesis of  $\text{Ru}^{\text{II}}$  precursors. Reagents and conditions: i)  $\text{RuCl}_3 \cdot x\text{H}_2\text{O}$ ; EtOH, 80 °C, overnight; ii) MeCN; EtOH,  $\text{H}_2\text{O}$ ; 80 °C, overnight.



Scheme 4. Synthesis of final complexes. Reagents and conditions: i) *n*BuOH, 130°C, overnight; ii) 1) BBr<sub>3</sub>; CH<sub>2</sub>Cl<sub>2</sub>, -78°C to room temperature, overnight; 2) 2,3-dichloro-5,6-dicyano-1,4-benzoquinone (DDO); acetone, room temperature, 3 h.

peak, but the masses observed for the peak show both the quinone and the hydroquinone. This may be an artefact of the ionization procedure, but one cannot rule out co-elution of the associated complexes. However, given the efforts made to exclude other impurities from the samples, it can be concluded that any observed long-lived components in the emission and transient absorption spectra can be assigned to residual hydroquinone present in the sample.

**Electrochemistry:** The redox properties of the dyad and triad complexes in dry MeCN were studied by cyclic voltammetry (CV) and differential pulse voltammetry (DPV). The electrochemical data are collected in Table 1. Half-wave potentials ( $E_{1/2}$ ) were determined by CV as the average of the anodic and cathodic peak potentials ( $E_{1/2} = (E_{pa} + E_{pc})/2$ ). Adsorption spikes were observed in the voltammograms after reduction to neutral or negative overall charge. For cases in which the CV waves were perturbed by these effects, half-wave potentials were determined from DPV peak potentials. The assignments given in Table 1 are based on comparison with literature values for [Ru(dqp)<sub>2</sub>]<sup>2+</sup> complexes and similar triads.

**Photochemistry:** The electronic absorption and emission spectra of the triads **1a** and **3a** are shown in Figure 2. The spectra of dyads **2a** and **4a**, and of the DMB reference com-

plexes **1b–4b**, are very similar and can be found in the Supporting Information. Electronic absorption and emission data for all complexes are summarized in Table 2, along with the results from time-resolved emission and transient absorption studies.

By comparison with the absorption spectrum of the parent complex [Ru(dqp)<sub>2</sub>]<sup>2+</sup>,<sup>[23]</sup> the broad band at 495 nm can be assigned to the lowest excited singlet MLCT state, and the higher bands (at 290 and 340 nm) are attributed to ligand-centred (LC) transitions. The small peak at 410 nm in the absorption spectrum of **1a** is found in all phenyl-linked complexes studied here (**1a**, **1b**, **2a** and **2b**). Complexes **3a**, **3b**, **4a** and **4b**, in which the dqp ligand is functionalized by an amide group, display increased absorption at 430 and 550 nm, similar to that previously observed for ester-functionalized [Ru(dqp)<sub>2</sub>]<sup>2+</sup>.<sup>[24]</sup>

The emission maximum shifts slightly with the different substituents (ca. 690–710 nm) and is assigned to a triplet MLCT (<sup>3</sup>MLCT) state origin, in analogy to [Ru(dqp)<sub>2</sub>]<sup>2+</sup>. Emission quantum yields, determined with [Ru(dqp)<sub>2</sub>]<sup>2+</sup> as a standard, are given in Table 2. The amide-functionalized complexes **3b** and **4b** display increased emission, in analogy to the documented observations for ester-functionalized [Ru(dqp)<sub>2</sub>]<sup>2+</sup>.<sup>[24]</sup> The emission quantum yields of **3a** and **4a** are evaluated versus their DMB references **3b** and **4b**, respectively.

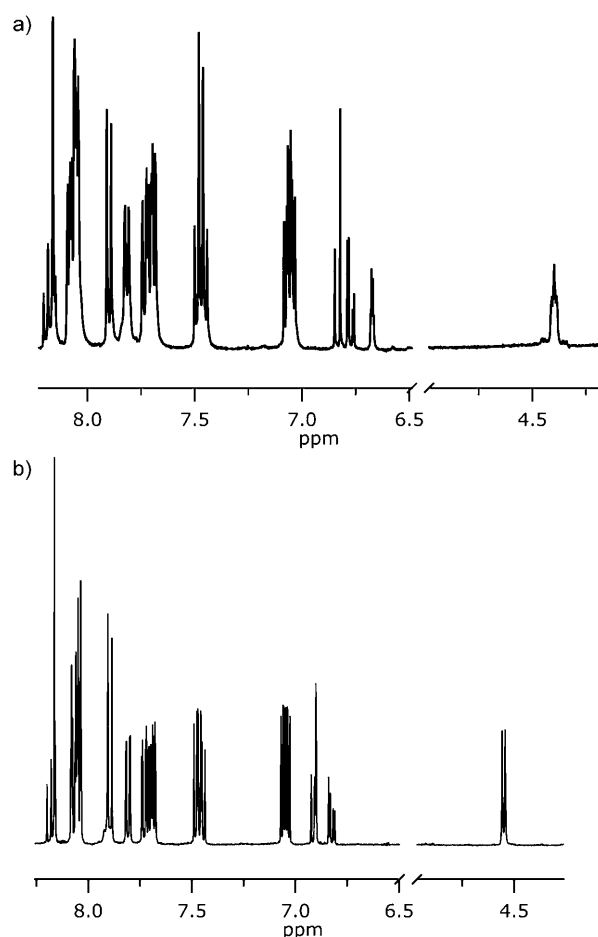


Figure 1.  $^1\text{H}$  NMR spectra of a) **1a** and b) **1b**. Shown is the aromatic region that contains differing chemical shifts in the case of a quinone ( $\delta=6.6\text{--}7.1$  ppm) or DMB motif ( $\delta=6.8\text{--}7.1$  ppm). Also shown is the  $\text{CH}_2$  unit alpha to the amide bond ( $\sim 4.5$  ppm), which shows a doublet in the case of an aromatic system but an allylic coupling for the quinone.

The  $^3\text{MLCT}$  excited-state decay upon excitation by visible light was investigated by time-resolved emission and transient absorption. Complexes **1b–4b** all have long excited-

Table 1. Electrochemical data.

Complex <sup>[a]</sup>	$E_{1/2}^{[b]}$ ( $\Delta E_p^{[c]}$ ) [Ru(L) <sub>2</sub> ] <sup>2+/+</sup>	BQ <sup>-</sup> /BQ <sup>2-</sup>	BQ/BQ <sup>-</sup>	PTZ <sup>+</sup> /PTZ	[Ru(L) <sub>2</sub> ] <sup>3+/2+</sup>	DMB <sup>+</sup> /DMB
<b>1a</b>	-1.70 <sup>[d,e]</sup>	-1.52 (87) <sup>[d]</sup> , -1.52 <sup>[e]</sup>	-0.82 (184), <sup>[d]</sup> -0.80 <sup>[e]</sup>	0.40 (100)	0.71 (93)	–
<b>1b</b>	–	–	–	0.42 (94)	0.73 (92)	0.89 (68)
<b>2a</b>	-1.73 (59), <sup>[d]</sup> -1.71 <sup>[e]</sup>	-1.41 (171), <sup>[d]</sup> -1.45 <sup>[e]</sup>	-0.84 (69)	–	0.71 (60)	–
<b>2b</b>	-1.76 (58)	–	–	–	0.67 (63)	0.84 (63)
<b>3a</b>	-1.74 <sup>[d,e]</sup>	-1.41 <sup>[d,e]</sup>	-0.78 (165), <sup>[d]</sup> -0.78 <sup>[e]</sup>	0.38 (80)	0.73 (87)	–
<b>3b</b>	-1.70 (61)	–	–	0.40 (60)	0.72 (64)	0.87 (90)
<b>4a</b>	-1.80 (67), <sup>[d]</sup> -1.69 <sup>[e]</sup>	-1.52 <sup>[d,e]</sup>	-0.84 (143), <sup>[d]</sup> -0.89 <sup>[e]</sup>	–	0.71 (68)	–
<b>4b</b>	-1.68 (57)	–	–	–	0.72 (59)	0.88 (83)

[a] Ionic complexes as  $\text{PF}_6^-$  salts. [b] V versus ferrocenium/ferrocene ( $\text{Fc}^{+/0}$ ) in MeCN, 0.1 M  $\text{Bu}_4\text{N}(\text{PF}_6)$ . [c] mV,  $v=0.1$  mV s<sup>-1</sup>. [d] Irreversible or poorly defined reverse wave. [e] Potential from DPV peak.

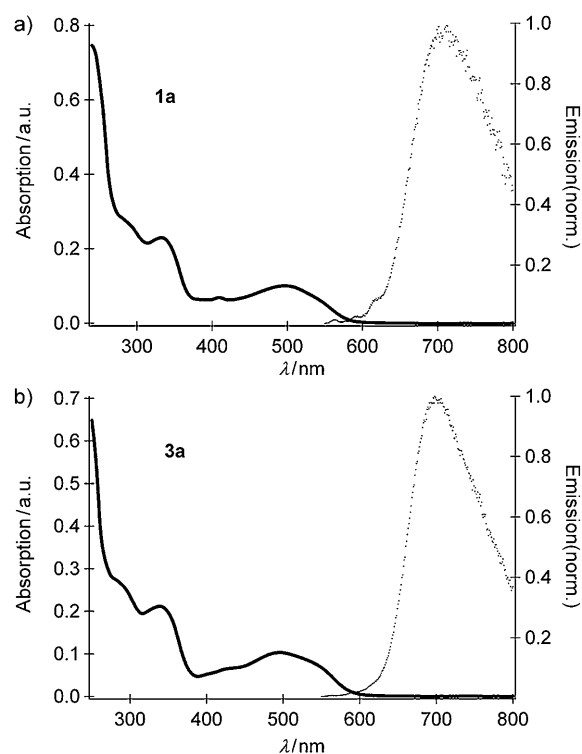


Figure 2. Electronic absorption (left scale) and emission (right scale) spectra for a) **1a** and b) **3a** in MeCN at 298 K. Emission spectra were collected in deaerated solutions and are normalized at maximum peak intensity.

state lifetimes of 2.7–3.5  $\mu\text{s}$  (Table 2), similar to the lifetime of  $[\text{Ru}(\text{dqp})_2]^{2+}$ . On the other hand, the quinone-containing complexes **1a–4a** are significantly quenched, as observed in both the emission yield and time-resolved emission measurements. Their  $^3\text{MLCT}$  excited-state lifetimes upon 400 nm excitation were determined by time-correlated single-photon counting. The emission lifetimes reported in Table 2 correspond to excited-state quenching rate constants of  $k_q(\mathbf{1a})=1.1\times 10^9$ ,  $k_q(\mathbf{2a})=1.1\times 10^9$ ,  $k_q(\mathbf{3a})=8.3\times 10^8$  and  $k_q(\mathbf{4a})=5.9\times 10^8$  s<sup>-1</sup>. All the complexes **1a–4a** also show

long-lived unquenched emission assigned to the corresponding hydroquinone complexes, as discussed above. These account for most of the emission quantum yields.

The transient absorption spectra upon 480 nm excitation of the dyads **2a** and **4a** (complex **2a** shown in Figure 3) show a MLCT ground-state bleach at about 500 nm and broad excited-state absorption bands at 400 and 600–650 nm, in excellent agreement with the  $[\text{Ru}(\text{dqp})_2]^{2+}$  excited-state features.<sup>[24]</sup> There are two isosbes-

Table 2. Photophysical and electron-transfer data at 298 K.

Complex <sup>[a]</sup>	Absorption (MLCT)		Emission (MLCT)			Electron transfer	
	$\lambda_{\max}$ [nm]	$\lambda_{\max}$ <sup>[b]</sup> [nm]	$\Phi_{\text{em}}$ <sup>[b]</sup>	$\tau_{\text{em}}$ [ns]	$k_{\text{CS}}$ <sup>[c]</sup> [s <sup>-1</sup> ]	$k_{\text{CR}}$ [s <sup>-1</sup> ]	
<b>1a</b>	497	708	0.002	0.91	$1.0 \times 10^9$	$5.0 \times 10^6$	
<b>1b</b>	497	708	0.02	2700 <sup>[b]</sup>	–	–	
<b>2a</b>	495	714	0.005	0.88	$1.1 \times 10^9$	$\geq 1 \times 10^9$	
<b>2b</b>	495	703	0.02	2900 <sup>[b]</sup>	–	–	
<b>3a</b>	496	698	0.02	1.2	$5.2 \times 10^8$	$7.1 \times 10^6$	
<b>3b</b>	495	701	0.05	2700 <sup>[b]</sup>	–	–	
<b>4a</b>	492	688	0.006	1.7	$5.1 \times 10^8$	$\geq 5 \times 10^8$	
<b>4b</b>	494	689	0.05	3500 <sup>[b]</sup>	–	–	
[Ru(dqp) <sub>2</sub> ] <sup>2+</sup> <sup>[d]</sup>	490	700	0.02	3000	–	–	

[a] Ionic complexes as PF<sub>6</sub><sup>-</sup> salts in MeCN. [b] Deaerated MeCN. [c] From ultrafast transient absorption measurements, 480 nm excitation. [d] Values from Abrahamsson et al.<sup>[24]</sup>

remaining excited-state features.<sup>[40]</sup> The difference spectra thus obtained clearly show the signatures of the Q<sup>-</sup> and PTZ<sup>+</sup> radicals around 440 and 510 nm, respectively.<sup>[41–44]</sup> This finding is interpreted as the signature of the fully charge-separated state PTZ<sup>+</sup>Ru<sup>II</sup>Q<sup>-</sup>.

Transient absorption traces for the excited-state decay (at 400 and 600 nm), ground-state recovery/Q<sup>-</sup> build-up (450 nm)

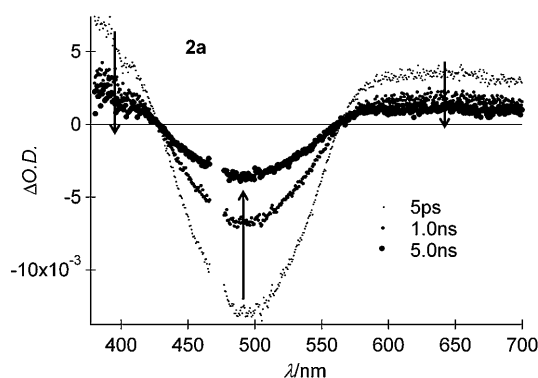


Figure 3. Transient absorption spectra at representative times for **2a** in MeCN at 298 K upon excitation by ~120 fs pulses at 480 nm. O.D.: optical density.

tic points at 427 and 564 nm, and thus it is likely that only two states (excited state and ground state) contribute to the transient spectra. Still, both **2a** and **4a** are significantly quenched compared to their DMB analogues **2b** and **4b**. The most likely quenching mechanism is that of electron transfer from the excited [Ru(dqp)<sub>2</sub>]<sup>2+</sup> moiety to the quinone, as discussed further below. If the rate of charge recombination ( $k_{\text{CR}}$ ) to the ground state is very fast ( $k_{\text{CR}} \gg k_{\text{CS}}$ ;  $k_{\text{CS}}$  is the rate of charge separation), the effective population of the charge-separated state will be very small and it will not be detected in the transient absorption spectra. The excited-state features decay with  $k_{\text{CS}}(\mathbf{2a}) = 1.1 \times 10^9$  and  $k_{\text{CS}}(\mathbf{4a}) = 5.1 \times 10^8 \text{ s}^{-1}$ , which matches the quenching rates from emission measurements well. The rate of charge separation was observed to vary slightly with the water content in the solvent, but we did not pursue systematic investigation of this effect.

In the transient absorption of the triads **1a** and **3a** (Figure 4), the initial spectra are identical to the excited-state spectra observed for **2a** and **4a**. At longer times, however, positive features grow at 450 and 510 nm simultaneously with the ground-state recovery. This state is still growing at 5 ns, which is the longest delay obtained in our ultrafast experiments. The insets in Figure 4 show the difference between the almost fully developed spectra (at 5 ns) and the

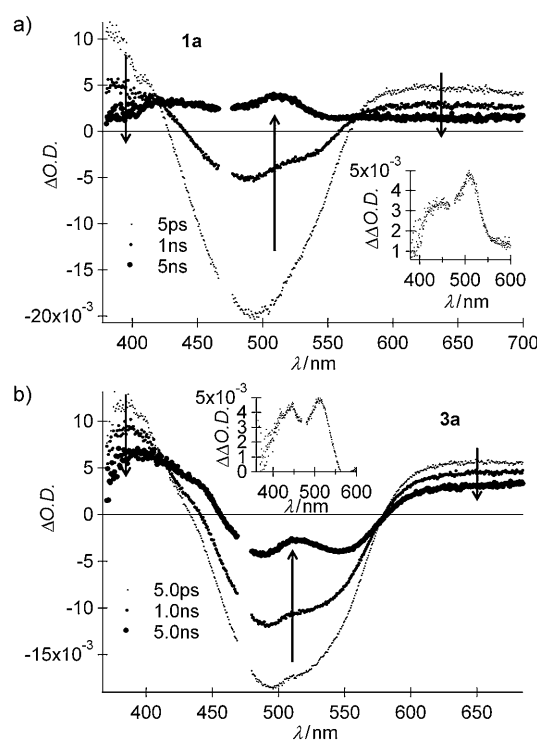


Figure 4. Transient absorption spectra for a) **1a** and b) **3a** in MeCN at 298 K upon excitation by ~120 fs pulses at 480 nm. Insets: the respective difference spectra at 5 ns, in which the excited-state features have been subtracted (see ref. [40]).

and ground-state recovery/growth of PTZ<sup>+</sup> (510 nm) of **1a** and **3a** are shown in Figure 5. The concomitant growth of the Q<sup>-</sup> and PTZ<sup>+</sup> signatures and decay of the [Ru(dqp)<sub>2</sub>]<sup>2+</sup>\* excited state was fitted to rate constants of  $k_{\text{CS}}(\mathbf{1a}) = 1.0 \times 10^9$  and  $k_{\text{CS}}(\mathbf{3a}) = 5.2 \times 10^8 \text{ s}^{-1}$ , respectively, in global fits at five to ten wavelengths. This is interpreted as the rate of formation of the charge-separated state PTZ<sup>+</sup>Ru<sup>II</sup>Q<sup>-</sup>. These rates correlate well with the quenching rates ( $k_{\text{q}}$ ) determined by time-resolved emission spectroscopy. An offset ( $k \ll 1.0 \times 10^8 \text{ s}^{-1}$ ) was also needed to fit the data, which corresponded in part to the long-lived charge-separated state, and which does not decay on the 10 ns timescale.

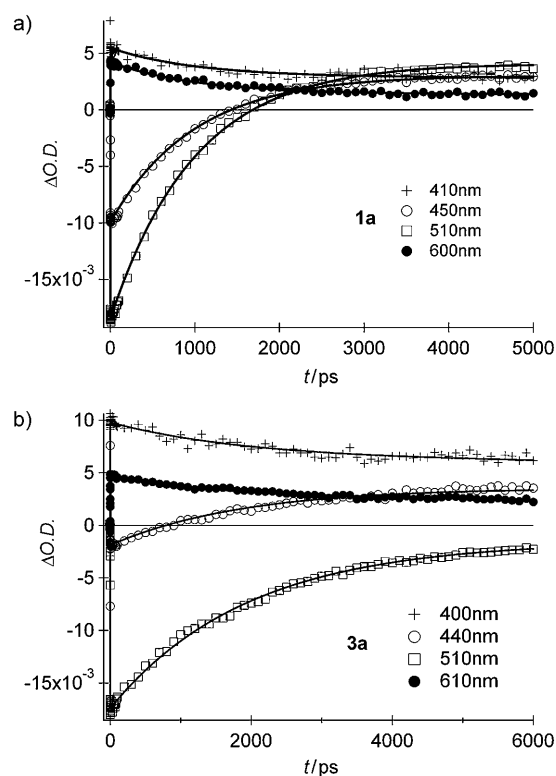


Figure 5. Transient absorption decay for a) **1a** and b) **3a** in MeCN at 298 K upon excitation by  $\sim 120$  fs pulses at 480 nm with global fits (solid lines).

The lifetime of the charge-separated state  $\text{PTZ}^+\text{Ru}^{\text{II}}\text{Q}^-$  in **1a** and **3a** was investigated by transient absorption spectroscopy on the nanosecond to microsecond timescale by 480 nm excitation pulses of  $\sim 8$  ns duration. The resulting spectra at representative times are found in the Supporting Information. The initial spectrum matches well the last spectrum in the ultrafast measurements (5 ns). As seen in Figure 6, the  $\text{Q}^-$  (440 nm) and  $\text{PTZ}^+$  (510/520 nm) signatures decay within  $< 1 \mu\text{s}$ , and a global fit at five wavelengths gives charge recombination rate constants of  $k_{\text{CR}}(\mathbf{1a}) = 5.0 \times 10^6$  and  $k_{\text{CR}}(\mathbf{3a}) = 7.1 \times 10^6 \text{ s}^{-1}$ . In line with the emission and ultrafast transient absorption measurements, an additional decay component attributed to the presence of unquenched hydroquinone triads ( $\tau \approx 3 \mu\text{s}$ ) also came out of the global fit. The charge recombination as such is single exponential, as can be expected for triads with only one geometrical isomer.

The energy of the lowest triplet excited state of benzoquinone in polar solvents is  $\geq 2.35$  eV according to the literature.<sup>[35]</sup> Thus, energy transfer from the  $^3\text{MLCT}$  excited state ( $E_{00} = 1.84$  eV for  $[\text{Ru}(\text{dqp})_2]^{2+}$  in a MeOH/EtOH glass)<sup>[23]</sup> to form the quinone triplet is a considerably uphill process, and not a likely quenching mechanism. From the electrochemistry data given in Table 1, the driving force for the electron transfer is approximately  $\Delta G_{\text{ET}}^0(\mathbf{2a}, \mathbf{4a}) = -0.3$  eV in the dyads, and for complete charge separation in the triads  $\Delta G_{\text{ET}}^0(\mathbf{1a}) = -0.6$  eV and  $\Delta G_{\text{ET}}^0(\mathbf{3a}) = -0.7$  eV.<sup>[45]</sup>

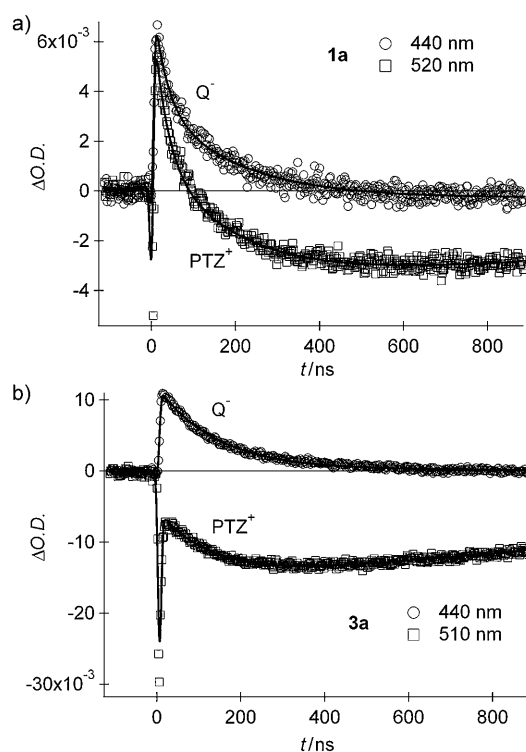
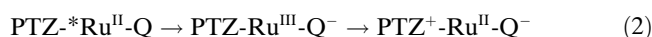
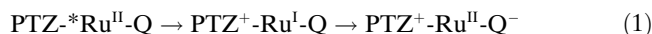


Figure 6. Charge recombination kinetics monitored by nanosecond transient absorption spectroscopy following the decay of  $\text{Q}^-$  at 440 nm and of  $\text{PTZ}^+$  at 520/510 nm for a) **1a** and b) **3a** in deaerated MeCN at 298 K. Global fits (solid lines) give charge-separated-state lifetimes of a) 140 and b) 200 ns.

In principle, the  $\text{PTZ}^+\text{Ru}^{\text{II}}\text{Q}^-$  charge-separated state could be formed through two alternative routes, reductive quenching [Eq. (1)] and oxidative quenching [Eq. (2)]:



The reductive quenching [Eq. (1)] would involve population of the  $\text{PTZ}^+\text{Ru}^{\text{I}}\text{Q}$  charge-separated state, which is thermodynamically uphill from the  $^3\text{MLCT}$  excited state ( $\Delta G_{\text{ET}}^0(\mathbf{1a}, \mathbf{3a}) = +0.3$  eV, as calculated from the redox potentials in Table 1;<sup>[46]</sup> see Figure 7). No quenching was observed for the DMB-substituted triad complexes **1b** and **3b** (see Table 2 and the Supporting Information). Instead, the overall rates of charge separation in **1a** and **3a** are very similar to the charge separation rate of the corresponding dyads **2a** and **4a**, respectively. Thus, it was concluded that the mechanism is electron transfer through the  $\text{PTZRu}^{\text{III}}\text{Q}^-$  charge-separated state [Eq. (2)]. This step is apparently the rate-determining one, followed by a very fast hole transfer to form the  $\text{PTZ}^+\text{Ru}^{\text{II}}\text{Q}^-$  state. Assuming that the charge recombination for the first charge-separated state in **1a** and **3a** is as rapid as in dyads **2a** and **4a**, this means that the yield of overall charge separation is strongly dependent on the rate of hole transfer to PTZ, which has to out-compete the charge recombination from the  $\text{PTZRu}^{\text{III}}\text{Q}^-$  state.

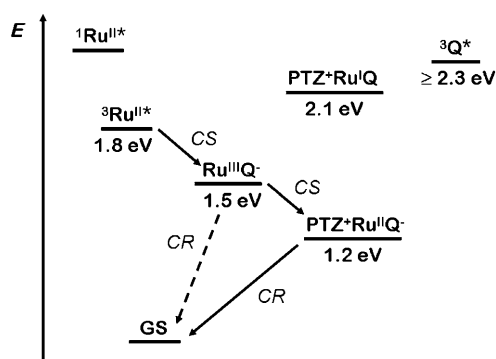


Figure 7. Schematic energy diagram of relevant excited and charge-separated states versus the ground state (GS) for the triads **1a** and **3a**. Triplet excited-state energies are taken from the literature.<sup>[23,35]</sup> The charge-separated-state energies are calculated from data in Table 1, as described in the text. Solid arrows mark the observed charge-separation (CS) and charge-recombination (CR) processes.

In multi-step electron transfer, there is competition between the charge recombination and further charge shift after the primary charge separation, in which fast recombination can decrease the total yield of charge separation. Examples of  $[\text{Ru}(\text{bpy})_3]^{2+}$ -based triads for which the overall yield is high ( $\geq 80\%$ ) have been reported.<sup>[30,47–49]</sup> In general, however, the overall yields of charge separation in  $\text{Ru}^{\text{II}}$  polypyridyl-based D-P-A assemblies given in the literature are moderate ( $\leq 40\%$ ).<sup>[14,16,50–52]</sup> For bis-tridentate motifs such as  $[\text{Ru}(\text{tpy})_2]^{2+}$ , the reported yields are very low, in large extent due to the short room-temperature lifetime of the chromophore.<sup>[18,53]</sup>

The yield of the fully charge-separated state  $\text{PTZ}^+\text{Ru}^{\text{II}}\text{Q}^-$  was evaluated from the spectroscopic signatures in the difference spectra at 5 ns (see Figure 4a and b, insets). The excited-state versus ground-state molar absorption coefficient of  $[\text{Ru}(\text{dqp})_2]^{2+}$  in MeCN was found to be  $\Delta\epsilon_{500}([\text{Ru}^{\text{II}}(\text{dqp})_2^*]) = -1.1 \times 10^4 \text{ M}^{-1} \text{ cm}^{-1}$ .<sup>[54]</sup> Several sources give  $\epsilon_{430}(\text{Q}^-) = 7 \times 10^3 \text{ M}^{-1} \text{ cm}^{-1}$  for the unprotonated benzoquinone radical.<sup>[30,43,44,55]</sup> On the other hand, the protonated semiquinone radical has a slightly blue-shifted peak with lower extinction coefficient ( $\epsilon_{415}(\text{QH}) = 4 \times 10^3 \text{ M}^{-1} \text{ cm}^{-1}$ ).<sup>[43,44,55]</sup> We cannot rule out that the benzoquinone radical is protonated to some degree, considering the indications that the rate of charge separation is sensitive to the water content in the solvent (see above). At this point, we did not investigate this aspect systematically, but rather base our evaluation of the charge-separated-state yield on the  $\text{PTZ}^+$  radical signature. The molar absorption coefficient of the oxidized PTZ in MeCN given in the literature is  $\epsilon_{515}(\text{PTZ}^+) = 5 \times 10^3 \text{ M}^{-1} \text{ cm}^{-1}$ .<sup>[51]</sup> By using this value, we estimate the overall yield of charge separation to be  $\geq 50\%$  in **1a** and  $\geq 95\%$  in **3a**.<sup>[56]</sup> These are remarkably high yields considering the very fast charge recombination ( $k_{\text{CR}} \gg k_{\text{CS}}$ ) of the first charge-separated state  $\text{PTZRu}^{\text{III}}\text{Q}^-$ . Apparently, the electron transfer from PTZ to the oxidized  $\text{Ru}^{\text{III}}$  moiety is approximately as fast or up to nine times faster than the charge recombination. Rapid electron transfer from PTZ

has been observed before in other  $\text{Ru}^{\text{II}}$  polypyridyl-based triads with comparable yields.<sup>[30,47–49]</sup>

Complexes **1a** and **3a** are the first examples known to us in which D-P-A triads based on bis-tridentate  $\text{Ru}^{\text{II}}$  polypyridyl motifs give such high yields of charge separation. Perhaps more outstanding than the fast hole transfer from PTZ is the high yield of formation of the primary charge separation (almost unity). The  $[\text{Ru}(\text{dqp})_2]^{2+}$  unit and its intrinsic long excited-state lifetime makes this possible, as the yield of electron transfer no longer suffers from the same kinetic limitations as with the  $[\text{Ru}(\text{tpy})_2]^{2+}$  or similar motifs. Notably, the overall yield for **3a** is among the highest reported in the literature for  $\text{Ru}^{\text{II}}$  polypyridyl-based triads (quoted above), which makes the  $[\text{Ru}(\text{dqp})_2]^{2+}$  motif a potent competitor to  $[\text{Ru}(\text{bpy})_3]^{2+}$  in D-P-A triad assemblies for photoinduced charge separation. Additionally, the  $[\text{Ru}(\text{dqp})_2]^{2+}$  unit enables a rodlike arrangement and does not introduce the same stereoisomeric heterogeneity in D-P-A assemblies as tris-bidentate complexes such as  $[\text{Ru}(\text{bpy})_3]^{2+}$ . This point was illustrated by the single exponential charge recombination in **1a** and **3a**. There is but one donor–acceptor distance, and the electron moves vectorially from one point in three-dimensional space to another. In all, these combined properties make triads **1a** and **3a** remarkable examples in the  $\text{Ru}^{\text{II}}$  polypyridyl family for vectorial electron transfer.

## Conclusions

We have presented the very first examples of D-P-A triads based on  $[\text{Ru}(\text{dqp})_2]^{2+}$ , **1a** and **3a**. The complexes were synthesized in good yield by adopting the convergent strategy of stepwise coordination of functionalized dqp ligands via a well-characterized  $[\text{Ru}(\text{R}^i\text{-dqp})(\text{MeCN})_3]^{2+}$  intermediate. Upon visible excitation, the excited  $[\text{Ru}(\text{dqp})_2]^{2+}$  <sup>3</sup>MLCT state is formed and subsequently quenched by electron transfer, which results in the  $\text{PTZ}^+\text{Ru}^{\text{II}}\text{Q}^-$  charge-separated state in high overall yields,  $\geq 50\%$  for complex **1a** and  $\geq 95\%$  for **3a**. To our knowledge, these are the highest yields of overall charge separation reported for bis-tridentate  $\text{Ru}^{\text{II}}$  polypyridyl assemblies. This is to a large extent ascribed to the intrinsically long lifetime of the  $[\text{Ru}(\text{dqp})_2]^{2+}$  MLCT excited state. The kinetics of charge recombination are monoexponential, as a consequence of the well-defined donor–acceptor distance stemming from the bis-tridentate  $[\text{Ru}(\text{dqp})_2]^{2+}$  motif. The long-lived charge-separated state ( $\tau_{\text{CS}}(\mathbf{1a}) = 140$ ,  $\tau_{\text{CS}}(\mathbf{3a}) = 200$  ns) and the vectorial electron transfer make these complexes very promising candidates for further studies towards artificial photosynthesis and electron transfer in molecular arrays.

## Experimental Section

NMR spectra were recorded on a JEOL spectrometer at 293 K. <sup>1</sup>H NMR spectra were recorded at 400 MHz and <sup>15</sup>C NMR spectra were recorded

at 101 Hz; chemical shifts are given in ppm and referenced internally to the residual solvent signal, and all coupling constants are in hertz. Microwave heating was performed in an Initiator single-mode microwave cavity at 2450 MHz (Biotage). Flash chromatography was detected by TLC (254 nm UV light) or visual inspection. Automated flash chromatography was performed on a Biotage SP4 system and detected at 254 and 310 nm by using pre-packed 50–100 g silica columns. High-resolution ESIMS was performed on a superconducting 9.4 T Fourier transform ion cyclotron resonance (FTICR) mass spectrometer equipped with an in-house-developed emitter. HPLC–MS data were obtained on a Dionex Ultimate 3000 system on a Phenomenex Gemini C18 column (150 × 3.0 mm, 5 μm) coupled to a Thermo LCQ Deca XP spectrometer with electrospray ionization (ESI). Solvents used for HPLC: 0.05% HCO<sub>2</sub>H in H<sub>2</sub>O and 0.05% HCO<sub>2</sub>H in MeCN. Preparative HPLC was performed on a C18 column (150 × 21.2 mm, 10 μm) with the indicated eluents. Electrochemical experiments were performed with a three-electrode set-up in a three-compartment cell connected to an Autolab potentiostat with a general-purpose electrochemical system (GPES) electrochemical interface (Eco Chemie). The working electrode was a glassy carbon disc (diameter 3 mm, freshly polished). Potentials were measured versus a non-aqueous Ag/Ag<sup>+</sup> reference electrode (CH Instruments, 10 mm AgNO<sub>3</sub> in MeCN) with a potential of –0.080 V versus the ferrocenium/ferrocene (Fc<sup>+/0</sup>) couple in MeCN.

All starting materials were purchased from Aldrich (St. Louis, USA) and used as received. [Ru(dqp)(MeCN)<sub>3</sub>](PF<sub>6</sub>)<sub>2</sub> was synthesized according to the literature procedure.<sup>[26]</sup>

**2,6-Dichloro-*N*-(2,5-dimethoxybenzyl)isonicotinamide (6):** 2,6-Dichloroisonicotinic acid (**5**, 1.3 g, 6.7 mmol), 2,5-dimethoxybenzylamine (1.2 g, 7.5 mmol), DCC (1.5 g, 7.5 mmol) and *N*-hydroxysuccinimide (0.78 g, 6.8 mmol) were stirred in CH<sub>2</sub>Cl<sub>2</sub> (30 mL) at room temperature. The solution was stirred for 3 h before being filtered, washed with H<sub>2</sub>O and concentrated in vacuo. The crude product was then purified by flash chromatography (SiO<sub>2</sub>, CH<sub>2</sub>Cl<sub>2</sub>, 1% CH<sub>3</sub>OH) to give **6** (1.8 g, 5.3 mmol, 78% yield) as a white solid. <sup>1</sup>H NMR (CDCl<sub>3</sub>): δ = 7.54 (s, 2H), 6.90–6.77 (m, 4H), 4.57 (d, *J* = 5.8 Hz, 2H), 3.85 (s, 3H), 3.76 ppm (s, 3H); <sup>13</sup>C NMR (CDCl<sub>3</sub>): δ = 162.6, 153.6, 151.7, 151.4, 147.1, 125.8, 120.7, 116.2, 113.5, 111.5, 55.9, 55.7, 40.6 ppm; LC–MS (ESI): *m/z*: calcd for C<sub>15</sub>H<sub>15</sub>Cl<sub>2</sub>N<sub>2</sub>O<sub>3</sub><sup>+</sup>: 341.0 [M+H]<sup>+</sup>; found: 341.0; retention time (r.t.): 10.09 min.

***N*-(2,5-Dimethoxybenzyl)-2,6-di(quinolin-8-yl)isonicotinamide (7):** Degassed H<sub>2</sub>O (2 mL) and MeCN (2 mL) were added to a mixture of **6**, 8-quinolinyboronic acid (1.0 g, 5.8 mmol), K<sub>2</sub>CO<sub>3</sub> (1.1 g, 7.9 mmol), SPhos (0.054 g, 0.13 mmol) and [Pd(dba)<sub>2</sub>] (0.076 g, 0.13 mmol). The suspension was then stirred and degassed for a further 5 min before being heated to 130 °C for 1 h by microwave heating. The solution was diluted with CH<sub>2</sub>Cl<sub>2</sub>, filtered and washed with H<sub>2</sub>O before being concentrated in vacuo. The product was purified by automated flash chromatography (SiO<sub>2</sub>, hexane, EtOAc 10–90%) to give **7** (1.0 g, 1.9 mmol, 72% yield) as an off-white solid. <sup>1</sup>H NMR (CDCl<sub>3</sub>): δ = 8.97 (dd, *J* = 1.7, 4.1 Hz, 2H), 8.46 (d, *J* = 9.3 Hz, 2H), 8.30 (m, 2H), 8.24 (dd, *J* = 1.7, 8.3 Hz, 2H), 7.90 (dd, *J* = 1.2, 8.1 Hz, 2H), 7.67 (t, *J* = 7.7 Hz, 2H), 7.46 (dd, *J* = 4.2, 8.3 Hz, 2H), 7.00–6.75 (m, 3H), 4.68 (d, *J* = 5.9 Hz, 2H), 3.83 (s, 3H), 3.76 ppm (s, 3H); <sup>13</sup>C NMR (CDCl<sub>3</sub>): δ = 166.5, 157.8, 153.8, 152.0, 150.5, 146.1, 141.2, 138.8, 136.7, 131.8, 129.1, 128.8, 127.1, 126.8, 123.2, 121.3, 116.1, 113.6, 111.5, 56.1, 56.0, 40.5 ppm; LC–MS (ESI): *m/z*: calcd for C<sub>33</sub>H<sub>27</sub>N<sub>4</sub>O<sub>3</sub><sup>+</sup>: 527.2 [M+H]<sup>+</sup>; found: 528.0; r.t.: 5.22 min.

**4-Bromo-2,6-dimethylbenzonitrile (9):** 4-Bromo-2,6-dimethylaniline (**8**, 4.5 g, 22.4 mmol) was taken up in H<sub>2</sub>O (25 mL) and HCl (37%, 8 mL) was added. The mixture was sonicated to form a fine suspension and then cooled to 0 °C. NaNO<sub>2</sub> (1.7 g, 24.2 mmol) in H<sub>2</sub>O (5 mL) was then added dropwise and the temperature maintained at 0 °C. The resulting solution was stirred at 0 °C for 30 min and then neutralized by the addition of solid NaHCO<sub>3</sub>. The resulting solution was added in portions to a stirred solution of CuCN (2.4 g, 27.0 mmol) and KCN (3.7 mL, 56.1 mmol) in H<sub>2</sub>O at 70 °C. The mixture was then stirred for 30 min, allowed to cool and extracted with toluene. The organic layer was washed with H<sub>2</sub>O and brine, dried and concentrated in vacuo. The crude residue was purified by flash chromatography (SiO<sub>2</sub>, hexane, 5% EtOAc) to give **9** (3.1 g, 14.76 mmol, 66% yield) as an off-white solid. <sup>1</sup>H NMR (CDCl<sub>3</sub>):

δ = 7.30 (s, 2H), 2.50 ppm (s, 6H); <sup>13</sup>C NMR (CDCl<sub>3</sub>): δ = 143.8, 130.5, 127.1, 116.6, 112.4, 20.5 ppm.

**4-Bromo-2,6-dimethylbenzaldehyde (10):** DIBAL-H (11.4 mL, 11.4 mmol) was added dropwise to a solution of **9** (2.0 g, 9.5 mmol) in CH<sub>2</sub>Cl<sub>2</sub> (20 mL) at 0 °C under an inert atmosphere. The solution was allowed to warm to room temperature and stirred overnight. The resulting solution was quenched with dilute HCl and heated at reflux for 30 min. The solution was extracted with CH<sub>2</sub>Cl<sub>2</sub> and the organic layers dried and concentrated in vacuo. The crude residue was purified by flash chromatography (SiO<sub>2</sub>, hexane, 10% EtOAc) to give **10** (1.6 g, 7.5 mmol, 79% yield). <sup>1</sup>H NMR (CDCl<sub>3</sub>): δ = 10.53 (s, 1H), 7.25 (s, 2H), 2.57 ppm (s, 6H); <sup>13</sup>C NMR (CDCl<sub>3</sub>): δ = 192.5, 142.9, 132.5, 131.1, 127.7, 20.3 ppm.

**4-(4-Bromo-2,6-dimethylphenyl)-2,6-di(quinolin-8-yl)pyridine (11):** 8-Acetylquinoline (1.28 g, 7.51 mmol) and **10** (0.8 g, 3.75 mmol) were dissolved in EtOH (4 mL). A solution of KOH (0.42 g, 7.51 mmol) in aqueous NH<sub>4</sub> (4 mL, 28%) was added. The reaction mixture was heated to 40 °C and stirred for 96 h before it was allowed to cool to room temperature, filtered and the obtained solid washed with EtOH. The solid was then purified by flash chromatography (SiO<sub>2</sub>, CH<sub>2</sub>Cl<sub>2</sub>, 4% MeOH) to give **11** (0.110 g, 0.213 mmol, 6% yield) as an off-white solid. <sup>1</sup>H NMR (CDCl<sub>3</sub>): δ = 8.94 (dd, *J* = 1.8, 4.1 Hz, 2H), 8.43 (dd, *J* = 1.5, 7.2 Hz, 2H), 8.21 (dd, *J* = 1.8, 8.3 Hz, 2H), 8.02 (s, 1H), 7.88 (dd, *J* = 1.4, 8.1 Hz, 2H), 7.69 (m, 2H), 7.42 (dd, *J* = 4.1, 8.3 Hz, 2H), 7.34 (s, 2H), 2.36 ppm (s, 6H); <sup>13</sup>C NMR (CDCl<sub>3</sub>): δ = 156.6, 150.2, 146.1, 145.9, 139.2, 138.6, 136.4, 131.6, 130.4, 128.7, 126.8, 126.7, 121.3, 121.0, 21.1 ppm; LC–MS (ESI): *m/z*: calcd for C<sub>31</sub>H<sub>23</sub>BrN<sub>3</sub><sup>+</sup>: 516.1 [M+H]<sup>+</sup>; found: 516.7; r.t.: 8.04 min.

**4-(2,5'-Dimethoxy-3,5-dimethylbiphenyl-4-yl)-2,6-di(quinolin-8-yl)pyridine (12):** 2,5-Dimethoxyphenylboronic acid (46.5 mg, 0.26 mmol), **11** (110 mg, 0.21 mmol), SPhos (4.4 mg, 10.6 μmol), [Pd(dba)<sub>2</sub>] (6.1 mg, 10.6 μmol) and K<sub>2</sub>CO<sub>3</sub> (44.2 mg, 0.32 mmol) were suspended in H<sub>2</sub>O (0.5 mL) and MeCN (0.5 mL). The solution was degassed for 5 min before being heated to 130 °C for 1 h by microwave heating. The crude mixture was diluted with CH<sub>2</sub>Cl<sub>2</sub> and the organic layer washed with H<sub>2</sub>O before being concentrated in vacuo. The crude residue was purified by flash chromatography (SiO<sub>2</sub>, CH<sub>2</sub>Cl<sub>2</sub>, 4% MeOH) to give **12** (75 mg, 0.13 mmol, 61% yield) as an off-white solid. <sup>1</sup>H NMR (CDCl<sub>3</sub>): δ = 8.95 (dd, *J* = 1.8, 4.2 Hz, 2H), 8.43 (dd, *J* = 1.5, 7.2 Hz, 2H), 8.22 (dd, *J* = 1.8, 8.3 Hz, 2H), 7.88 (dd, *J* = 1.5, 8.1 Hz, 2H), 7.70 (dd, *J* = 7.2, 8.1 Hz, 2H), 7.42 (dd, *J* = 4.1, 8.3 Hz, 2H), 7.35 (s, 2H), 6.91 (ddd, *J* = 3.0, 9.5, 11.9 Hz, 3H), 3.82 (s, 3H), 3.81 (s, 3H), 2.43 ppm (s, 6H); <sup>13</sup>C NMR (CDCl<sub>3</sub>): δ = 156.4, 153.7, 150.8, 150.1, 146.9, 146.0, 139.4, 138.9, 137.5, 136.2, 136.0, 131.4, 128.6, 128.6, 128.5, 127.0, 126.6, 120.9, 116.7, 113.1, 112.3, 56.3, 55.8, 21.3 ppm; LC–MS (ESI): *m/z*: calcd for C<sub>39</sub>H<sub>32</sub>N<sub>3</sub>O<sub>2</sub><sup>+</sup>: 574.2 [M+H]<sup>+</sup>; found: 574.4; r.t.: 8.06 min.

**Ethyl 2,6-dichloroisonicotinate (13):** Sulfuric acid (5.5 mL, 103 mmol) and **5** (3.3 g, 17.1 mmol) were mixed in EtOH (50 mL) to give a brown solution. The reaction vessel was heated to 80 °C for 2 h before the reaction mixture was poured onto ice (10 g) and filtered through a sintered glass funnel. The solid was partitioned between CH<sub>2</sub>Cl<sub>2</sub> and H<sub>2</sub>O, basified with NaHCO<sub>3</sub> and the layers were separated. The aqueous layer was extracted with CH<sub>2</sub>Cl<sub>2</sub> (3 × 25 mL) and the combined organic layers were dried over Na<sub>2</sub>SO<sub>4</sub>, filtered and concentrated. The crude product was purified by recrystallization from MeOH to give **13** (3.2 g, 14.5 mmol, 85% yield) as colourless needles. <sup>1</sup>H NMR (CDCl<sub>3</sub>): δ = 7.80 (s, 2H), 4.42 (q, *J* = 7.1 Hz, 2H), 1.41 ppm (t, *J* = 7.1 Hz, 3H); <sup>13</sup>C NMR (CDCl<sub>3</sub>): δ = 163.0, 151.7, 143.0, 122.9, 62.9, 14.3 ppm.

**(2,6-Dichloropyridin-4-yl)methanol (14):** NaBH<sub>4</sub> (2.7 g, 70.4 mmol) was added in portions over 5 min to a solution of **13** (3.1 g, 14.1 mmol) in EtOH (100 mL) at 0 °C. The resulting solution was heated to 80 °C for 3 h. The solution was then evaporated to dryness and taken up in H<sub>2</sub>O (80 mL). The excess NaBH<sub>4</sub> was then destroyed with 1 M HCl (20 mL) and the solution adjusted to pH 7 with aqueous saturated (sat.) Na<sub>2</sub>CO<sub>3</sub>. This solution was then extracted with CH<sub>2</sub>Cl<sub>2</sub> and the combined organic fractions concentrated in vacuo. The crude residue was purified by recrystallization from MeOH to give **14** (2.3 g, 12.9 mmol, 92% yield) as a white crystalline solid. Spectra were identical to those reported in the literature.<sup>[57]</sup>

**4-Hydroxymethyl-2,6-di(quinolin-8-yl)pyridine (15):** Degassed H<sub>2</sub>O (2 mL) and MeCN (2 mL) were added to a mixture of **14** (0.75 g, 4.2 mmol), 8-quinolinylboronic acid (1.6 g, 9.3 mmol), K<sub>2</sub>CO<sub>3</sub> (1.7 g, 12.6 mmol), SPhos (0.086 g, 0.21 mmol) and [Pd(dba)<sub>2</sub>] (0.12 g, 0.21 mmol). The suspension was then stirred and degassed a further 5 min before being heated to 130°C for 1 h by microwave heating. The solution was diluted with CH<sub>2</sub>Cl<sub>2</sub>, washed with H<sub>2</sub>O, dried with Na<sub>2</sub>SO<sub>4</sub> and concentrated in vacuo. The crude product was purified by automated flash chromatography (SiO<sub>2</sub>, hexane, EtOAc 10–90%) to give **15** (0.81 g, 2.215 mmol, 53% yield) as a white solid. <sup>1</sup>H NMR (CDCl<sub>3</sub>): δ = 8.90 (dd, *J* = 1.8, 4.2 Hz, 2H), 8.18 (dd, *J* = 1.8, 8.3 Hz, 2H), 8.13 (dd, *J* = 1.5, 7.2 Hz, 2H), 7.91 (s, 2H), 7.82 (dd, *J* = 1.5, 8.2 Hz, 2H), 7.59 (m, 2H), 7.38 (dd, *J* = 4.2, 8.3 Hz, 2H), 4.78 ppm (s, 2H); <sup>13</sup>C NMR (CDCl<sub>3</sub>): δ = 156.9, 150.1, 149.3, 145.8, 139.4, 136.5, 131.4, 128.6, 128.4, 126.5, 123.0, 120.9, 63.8 ppm; LC–MS (ESI): *m/z*: calcd for C<sub>24</sub>H<sub>18</sub>N<sub>3</sub>O<sup>+</sup>: 364.1 [M+H]<sup>+</sup>; found: 364.4; r.t.: 5.12 min.

**4-Bromomethyl-2,6-di(quinolin-8-yl)pyridine (16):** A solution of PBr<sub>3</sub> (0.48 mL, 5.0 mmol) in CH<sub>2</sub>Cl<sub>2</sub> (15 mL) was added dropwise to a stirred solution of **15** (1.5 g, 4.2 mmol) in CH<sub>2</sub>Cl<sub>2</sub> (15 mL) under an inert atmosphere at 0°C. The solution was allowed to warm to room temperature and stirred overnight. The solution was recooled to 0°C, quenched with H<sub>2</sub>O (30 mL), and the aqueous layer was basified with NaHCO<sub>3</sub> and extracted with CHCl<sub>3</sub>. The combined organic layers were dried with Na<sub>2</sub>SO<sub>4</sub> and concentrated in vacuo. The residue was purified by automated flash chromatography (SiO<sub>2</sub>, hexane, EtOAc 10–90%) to give **16** (1.7 g, 4.0 mmol, 94% yield) as a white solid. <sup>1</sup>H NMR (CDCl<sub>3</sub>): δ = 9.00 (dd, *J* = 1.8, 4.2 Hz, 2H), 8.29 (dd, *J* = 1.5, 7.2 Hz, 2H), 8.24 (dd, *J* = 1.8, 8.3 Hz, 2H), 8.18 (s, 2H), 7.89 (dd, *J* = 1.5, 8.1 Hz, 2H), 7.67 (m, 2H), 7.46 (dd, *J* = 4.2, 8.3 Hz, 2H), 4.67 ppm (s, 2H); <sup>13</sup>C NMR (CDCl<sub>3</sub>): δ = 157.3, 150.3, 145.9, 144.5, 138.8, 136.4, 131.6, 128.7, 128.6, 126.6, 125.6, 121.0, 32.0 ppm; LC–MS (ESI): *m/z*: calcd for C<sub>24</sub>H<sub>17</sub>BrN<sub>3</sub><sup>+</sup>: 426.1 [M+H]<sup>+</sup>; found: 426.3; r.t.: 6.2 min.

**10-[[2,6-Di(quinolin-8-yl)pyridin-4-yl]methyl]-phenothiazine (17):** 10H-PTZ (1.6 g, 7.8 mmol) in THF (10 mL) was added dropwise over 2 min to a suspension of NaH (60%, 0.3 g, 7.8 mmol) in THF (20 mL) at 0°C under an inert atmosphere. The solution was allowed to warm to room temperature and stirred for an additional 1 h before being recooled to 0°C. Then a solution of **14** (1.7 g, 3.9 mmol) in THF (5 mL) was added dropwise. The crude product was purified by flash chromatography (SiO<sub>2</sub>, hexane, EtOAc 50%) to give **17** (1.6 g, 2.9 mmol, 75% yield) as an off-white solid. <sup>1</sup>H NMR (CDCl<sub>3</sub>): δ = 8.81 (dd, *J* = 1.8, 4.1 Hz, 2H), 8.32 (dd, *J* = 1.5, 7.2 Hz, 2H), 8.18 (dd, *J* = 1.8, 8.3 Hz, 2H), 8.09 (s, 2H), 7.85 (dd, *J* = 1.5, 8.1 Hz, 2H), 7.65 (dd, *J* = 7.3, 8.1 Hz, 2H), 7.39 (dd, *J* = 4.2, 8.3 Hz, 2H), 7.08 (m, 4H), 6.90 (m, 4H), 5.30 ppm (s, 2H); <sup>13</sup>C NMR (CDCl<sub>3</sub>): δ = 225.3, 157.0, 150.2, 146.0, 144.7, 144.3, 139.1, 136.4, 131.6, 128.7, 128.7, 127.5, 126.7, 126.6, 124.0, 122.9, 122.6, 121.0, 116.0, 53.2 ppm; LC–MS (ESI): *m/z*: calcd for C<sub>36</sub>H<sub>25</sub>N<sub>4</sub>S<sup>+</sup>: 545.2 [M+H]<sup>+</sup>; found: 545.3; r.t.: 7.89 min.

**[Ru(7)(MeCN)<sub>3</sub>](PF<sub>6</sub>)<sub>2</sub> (18):** A solution of RuCl<sub>3</sub>·xH<sub>2</sub>O (248 mg, 0.95 mmol) and **7** (500 mg, 0.95 mmol) was heated at reflux in EtOH (25 mL) overnight. The resulting inorganic solid was isolated by filtration and washed with EtOH (3 × 10 mL) and Et<sub>2</sub>O (3 × 10 mL). The solid was dried in vacuo to give [Ru(7)Cl<sub>3</sub>] (630 mg, 0.86 mmol, 90% yield) as a green/brown solid. The crude product (630 mg, 0.86 mmol) was suspended in a mixture of H<sub>2</sub>O (5 mL), EtOH (5 mL) and MeCN (25 mL), and AgNO<sub>3</sub> (481 mg, 2.8 mmol) was added. The solution was stirred at 80°C for 5 h before being filtered through celite, washed with MeCN and concentrated in vacuo. The crude residue was purified by flash chromatography (SiO<sub>2</sub>, 40:4:1 MeCN/H<sub>2</sub>O/KNO<sub>3</sub> (sat.)) and isolated as the PF<sub>6</sub><sup>-</sup> salt to give **18** as a yellow solid (830 mg, 0.80 mmol, 84% yield over two steps). <sup>1</sup>H NMR (CD<sub>3</sub>CN): δ = 9.07 (dd, *J* = 5.1, 1.4 Hz, 2H), 8.63–8.60 (m, 4H), 8.28 (dd, *J* = 8.2, 1.2 Hz, 2H), 8.24 (s, 2H), 7.93 (dd, *J* = 8.1, 7.6 Hz, 2H), 7.85 (t, *J* = 5.8 Hz, 1H), 7.67 (dd, *J* = 8.2, 5.2 Hz, 2H), 6.92–6.79 (m, 3H), 4.55 (d, *J* = 5.8 Hz, 2H), 3.79 (s, 3H), 3.70 (s, 3H), 2.44 (s, 6H), 2.15 ppm (s, 3H); <sup>13</sup>C NMR (CD<sub>3</sub>CN): δ = 164.5, 159.8, 159.2, 154.6, 152.7, 147.2, 144.4, 139.8, 135.2, 135.2, 133.3, 129.7, 129.2, 128.1, 127.6, 126.2, 123.36, 116.7, 113.4, 112.7, 56.7, 56.3, 40.2, 4.6, 3.9 ppm; LC–MS

(ESI): *m/z*: calcd for C<sub>39</sub>H<sub>35</sub>N<sub>7</sub>O<sub>3</sub>Ru<sup>2+</sup> ([M<sup>2+</sup>]): 375.6; found: 375.4; r.t.: 4.02 min.

**[Ru(12)(MeCN)<sub>3</sub>](PF<sub>6</sub>)<sub>2</sub> (19):** Compound **19** was synthesized by the method used for **18** from RuCl<sub>3</sub>·xH<sub>2</sub>O (45.6 mg, 0.174 mmol) and **12** (100 mg, 0.174 mmol) to give **19** as a yellow solid (111 mg, 0.102 mmol, 66% yield). <sup>1</sup>H NMR (CD<sub>3</sub>CN): δ = 9.14 (dd, *J* = 1.4, 5.1 Hz, 2H), 8.62 (dd, *J* = 1.4, 8.3 Hz, 2H), 8.55 (dd, *J* = 1.2, 7.5 Hz, 2H), 8.26 (dd, *J* = 1.1, 8.2 Hz, 2H), 7.87 (m, 4H), 7.70 (dd, *J* = 5.2, 8.3 Hz, 2H), 7.37 (m, 1H), 6.96 (m, 3H), 3.79 (s, 3H), 3.75 (s, 3H), 2.21 (s, 9H), 1.99 ppm (s, 6H); <sup>13</sup>C NMR (CD<sub>3</sub>CN): δ = 159.6, 158.2, 154.8, 152.7, 151.7, 147.2, 139.9, 139.6, 137.1, 136.1, 135.2, 135.0, 132.8, 131.6, 129.8, 129.7, 129.6, 129.0, 127.3, 123.1, 117.3, 114.2, 113.8, 56.7, 56.3, 21.0, 4.4, 3.8 ppm; LC–MS (ESI): *m/z*: calcd for C<sub>45</sub>H<sub>40</sub>N<sub>6</sub>O<sub>2</sub>Ru<sup>2+</sup> ([M<sup>2+</sup>]): 399.1; found: 398.6; r.t.: 4.57 min.

**Complex 4b:** A suspension of **7** (46.6 mg, 0.088 mmol) and [Ru(dqp)-(MeCN)<sub>3</sub>](PF<sub>6</sub>)<sub>2</sub> (75 mg, 0.088 mmol) was vigorously heated at reflux in *n*BuOH (2 mL) overnight. The red solution was poured into aqueous NH<sub>4</sub>PF<sub>6</sub> and extracted with CH<sub>2</sub>Cl<sub>2</sub>. The organic phase was concentrated in vacuo and the crude residue purified by flash chromatography on silica gel (40:4:1 MeCN/H<sub>2</sub>O/KNO<sub>3</sub> (sat.)). Fractions containing the product were collected, concentrated in vacuo and diluted with aqueous NH<sub>4</sub>PF<sub>6</sub> before being extracted with CH<sub>2</sub>Cl<sub>2</sub>. The PF<sub>6</sub> salt was suspended in degassed MeOH/H<sub>2</sub>O (1:1) and Dowex 1 anion-exchange resin (Cl<sup>-</sup> form) was added. The suspension was then stirred for 3 h, filtered and concentrated in vacuo to give the chloride salt. This salt was then purified by preparative HPLC (isocratic elution with H<sub>2</sub>O, 45% MeOH, 50 mM NaHPO<sub>4</sub>, pH 7) before being isolated as the PF<sub>6</sub> salt as described above to give **4** (61 mg, 0.049 mmol, 55% yield) as a red solid. <sup>1</sup>H NMR (CD<sub>3</sub>CN): δ = 8.23–8.13 (m, 3H), 8.09–8.02 (m, 8H), 7.94–7.87 (m, 3H), 7.81 (dd, *J* = 7.5, 1.3 Hz, 2H), 7.76–7.65 (m, 4H), 7.52–7.42 (m, 4H), 7.09–7.00 (m, 4H), 6.95–6.87 (m, 2H), 6.86–6.78 (m, 1H), 4.55 (d, *J* = 5.9 Hz, 2H), 3.80 (s, 3H), 3.71 ppm (s, 3H); <sup>13</sup>C NMR (CD<sub>3</sub>CN): δ = 164.5, 159.5, 159.4, 158.6, 157.7, 154.5, 152.5, 147.4, 143.5, 139.3, 138.7, 134.3, 134.0, 132.7, 132.5, 131.8, 131.6, 129.0, 128.0, 127.8, 127.8, 127.6, 126.1, 123.1, 123.0, 116.7, 113.2, 112.6, 56.6, 56.2, 40.0 ppm; LC–MS (ESI): *m/z*: calcd for C<sub>36</sub>H<sub>41</sub>N<sub>7</sub>O<sub>3</sub>Ru<sup>2+</sup> ([M<sup>2+</sup>]): 480.6; found: 480.8; r.t.: 4.25 min.

**Complex 1b:** Prepared as for **4b** from **17** (61.8 mg, 0.102 mmol) and **19** (111 mg, 0.102 mmol), and purified by preparative HPLC (isocratic elution with H<sub>2</sub>O, 65% MeOH, 0.1% trifluoroacetic acid (TFA)) to give **1b** (77 mg, 0.051 mmol, 50% yield) as a red solid. <sup>1</sup>H NMR (CD<sub>3</sub>CN): δ = 8.18 (dd, *J* = 5.2, 1.4 Hz, 2H), 8.09–7.98 (m, 6H), 7.87 (s, 2H), 7.79 (s, 2H), 7.74 (dd, *J* = 7.4, 1.3 Hz, 2H), 7.69–7.63 (m, 4H), 7.47–7.34 (m, 8H), 7.26 (dd, *J* = 7.6, 1.5 Hz, 2H), 7.20–7.14 (m, 2H), 7.09–6.99 (m, 5H), 6.96–6.84 (m, 6H), 5.36 (q, *J* = 17.5 Hz, 2H), 3.78 (s, 3H), 3.74 (s, 3H), 2.19 ppm (s, 6H); LC–MS (ESI): *m/z*: calcd for C<sub>75</sub>H<sub>55</sub>N<sub>7</sub>O<sub>2</sub>RuS<sup>2+</sup> ([M<sup>2+</sup>]): 609.66; found: 609.50; r.t.: 5.18 min.

**Complex 2b:** Prepared as for **4b** from **12** (49.9 mg, 0.087 mmol) and [Ru(dqp)(MeCN)<sub>3</sub>](PF<sub>6</sub>)<sub>2</sub> (75 mg, 0.087 mmol), and purified by preparative HPLC (isocratic elution with H<sub>2</sub>O, 55% MeOH, 0.1% TFA) to give **2b** (32 mg, 0.025 mmol, 28% yield) as a red solid. <sup>1</sup>H NMR (CD<sub>3</sub>CN): δ = 8.23–8.15 (m, 3H), 8.12–8.06 (m, 6H), 7.91 (d, *J* = 8.1 Hz, 2H), 7.79 (s, 2H), 7.78–7.72 (m, 4H), 7.71–7.66 (m, 4H), 7.38–7.50 (m, 4H), 7.37 (s, 2H), 7.06 (ddd, *J* = 6.9, 10.6, 18.1 Hz, 5H), 6.91 (td, *J* = 2.9, 4.2 Hz, 2H), 3.79 (s, 3H), 3.75 (s, 3H), 2.20 ppm (s, 6H); <sup>13</sup>C NMR (CD<sub>3</sub>CN): δ = 159.5, 159.4, 157.9, 157.8, 154.7, 152.2, 151.6, 147.6, 139.8, 139.1, 138.6, 138.6, 137.1, 136.0, 134.4, 134.0, 132.8, 132.6, 131.6, 129.8, 129.6, 128.9, 127.8, 127.6, 127.5, 122.9, 117.4, 114.1, 113.7, 56.6, 56.2, 20.9 ppm; LC–MS (ESI): *m/z*: calcd for C<sub>62</sub>H<sub>46</sub>N<sub>6</sub>O<sub>2</sub>Ru<sup>2+</sup> ([M<sup>2+</sup>]): 504.1; found: 503.9; r.t.: 4.73 min.

**Complex 3b:** Prepared as for **4b** from **17** (209 mg, 0.384 mmol) and **18** (400 mg, 0.384 mmol), and purified by preparative HPLC (65% MeOH in H<sub>2</sub>O) to give **3b** (335 mg, 0.229 mmol, 60% yield) as a red solid. <sup>1</sup>H NMR (CD<sub>3</sub>CN): δ = 8.15 (s, 2H), 8.07–7.99 (m, 6H), 7.94 (dd, *J* = 5.2, 1.4 Hz, 2H), 7.85 (s, 2H), 7.84–7.76 (m, 3H), 7.69–7.62 (m, 4H), 7.49–7.36 (m, 6H), 7.25 (dd, *J* = 7.6, 1.5 Hz, 2H), 7.19–7.10 (m, 2H), 7.06–6.98 (m, 4H), 6.94–6.79 (m, 7H), 5.35 (q, *J* = 17.4 Hz, 2H), 4.55 (d, *J* = 5.9 Hz,

2H), 3.79 (s, 3H), 3.71 ppm (s, 3H); LC–MS (ESI):  $m/z$ : calcd for  $C_{60}H_{50}N_8O_3RuS^{2+}$  ( $[M^{2+}]$ ): 586.14; found: 586.26; r.t.: 4.90 min.

**Complex 4a:**  $BBr_3$  (1 M in hexanes, 1.6 mL, 1.6 mmol) was added dropwise to a solution of **4b** (40 mg, 0.032 mmol) in  $CH_2Cl_2$  (4 mL) under an inert atmosphere at  $-78^\circ C$ . The solution was allowed to warm slowly to room temperature overnight. The solution was then diluted with  $CH_2Cl_2$ , cooled to  $0^\circ C$  and quenched with aqueous  $NH_4PF_6$ . The organic layer was separated and the aqueous layer washed with  $CH_2Cl_2/10\%$  MeOH. The organic layers were combined and concentrated in vacuo before the crude residue was purified by flash chromatography on silica gel (40:4:1 MeCN/ $H_2O$ /KNO<sub>3</sub> (sat.)). Fractions containing the product were collected, concentrated in vacuo and diluted with aqueous  $NH_4PF_6$  before being extracted with  $CH_2Cl_2/10\%$  MeOH. The resulting solution was concentrated in vacuo to give the hydroquinone as a red solid. The product was dissolved in acetone (5 mL) at room temperature under an inert atmosphere and DDQ (35 mg, 0.155 mmol) was added. The resulting solution was stirred for 3 h. The solution was triturated with  $Et_2O$  to precipitate the product, which was collected by filtration and washed several times with  $Et_2O$  to remove DDQ. Complex **4a** (20 mg, 0.016 mmol, 52%) was obtained as a red solid and used without further purification.  $^1H$  NMR ( $CD_3CN$ ):  $\delta$  = 8.21–8.13 (m, 3H), 8.10–8.02 (m, 8H), 7.90 (d,  $J$  = 8.1 Hz, 2H), 7.85–7.77 (m, 3H), 7.76–7.65 (m, 6H), 7.47 (dd,  $J$  = 15.6, 7.8 Hz, 4H), 7.10–7.00 (m, 4H), 6.86–6.74 (m, 2H), 6.69–6.65 (m, 1H), 4.40 ppm (t,  $J$  = 4.1 Hz, 2H); HRMS (ESI-FTICR MS): calcd for  $C_{54}H_{35}N_7O_3Ru^{2+}$  ( $[M^{2+}]$ ): 465.592245; found: 465.58743; calcd for  $C_{54}H_{35}F_6N_7O_3PRu$ : 1076.14867  $[M+PF_6]^+$ ; found: 1076.10921; elemental analysis calcd (%) for  $C_{56}H_{30}Cl_4F_{12}N_7O_3P_2Ru$  (**4a**·2 $CH_2Cl_2$ ): C 48.36, H 2.83, N 7.05; found: C 48.33, H 3.09, N 7.40.

**Complex 1a:** Prepared as for **4a** from **1b** (70 mg, 0.046 mmol) to give **1a** (31 mg, 0.021 mmol, 46%) as a red solid.  $^1H$  NMR ( $CD_3CN$ ):  $\delta$  = 8.17 (dd,  $J$  = 5.2, 1.4 Hz, 2H), 8.08–7.98 (m, 6H), 7.86 (s, 2H), 7.77 (s, 2H), 7.72 (dd,  $J$  = 7.5, 1.3 Hz, 2H), 7.68–7.63 (m, 4H), 7.47–7.35 (m, 6H), 7.34 (s, 2H), 7.25 (dd,  $J$  = 7.6, 1.5 Hz, 2H), 7.20–7.13 (m, 2H), 7.08–6.99 (m, 4H), 6.95–6.84 (m, 7H), 5.35 (q,  $J$  = 17.4 Hz, 2H), 2.18 ppm (s, 6H); HRMS (ESI-FTICR MS): calcd for  $C_{73}H_{49}N_7O_2RuS^{2+}$  ( $[M^{2+}]$ ): 594.63559; found: 594.61664; calcd for  $C_{73}H_{49}F_6N_7O_2PRuS^{2+}$  ( $[M^{2+}]$ ): 1334.23537; found: 1334.18609; elemental analysis calcd (%) for  $C_{73}H_{49}F_{12}N_7O_2P_2RuS$ : C 59.27, H 3.34, N 6.63; found: C 59.33, H 3.58, N 6.41.

**Complex 2a:** Prepared as for **4a** from **2b** (20 mg, 0.015 mmol) to give **2a** (9.4 mg, 7 mmol, 49%) as a red solid.  $^1H$  NMR ( $CD_3CN$ ):  $\delta$  = 8.24–8.15 (m, 3H), 8.12–8.05 (m, 6H), 7.91 (d,  $J$  = 8.1 Hz, 2H), 7.78 (s, 2H), 7.76–7.71 (m, 4H), 7.71–7.65 (m, 4H), 7.49–7.37 (m, 4H), 7.37–7.33 (m, 2H), 7.12–7.04 (m, 4H), 6.92–6.83 (m, 3H), 2.21 ppm (s, 6H); HRMS (ESI-FTICR MS): calcd for  $C_{60}H_{40}N_6O_2Ru^{2+}$  ( $[M^{2+}]$ ): 489.11281; found: 489.12072; calcd for  $C_{60}H_{40}F_6N_6O_2PRu^{2+}$ : 1123.18980  $[M+PF_6]^+$ ; found: 1123.14751; elemental analysis calcd for  $C_{60}H_{40}F_{12}N_6O_2P_2Ru$  (**2a**): C 56.83, H 3.18, N 6.63; found: C 56.69, H 3.32, N 6.59.

**Complex 3a:** Prepared as for **4a** from **3b** (150 mg, 0.103 mmol) to give **3a** (61 mg, 0.042 mmol, 41%) as a red solid.  $^1H$  NMR ( $CD_3CN$ ):  $\delta$  = 8.19–8.14 (m, 2H), 8.08–7.98 (m, 6H), 7.97–7.91 (m, 3H), 7.87–7.77 (m, 4H), 7.70–7.62 (m, 4H), 7.49–7.36 (m, 6H), 7.27–7.21 (m, 2H), 7.18–7.12 (m, 2H), 7.08–6.98 (m, 4H), 6.95–6.88 (m, 2H), 6.87–6.82 (m, 2H), 6.81–6.60 (m, 3H), 5.43–5.27 (m, 2H), 4.48 (d,  $J$  = 6.1 Hz, 0.5H), 4.41–4.35 ppm (m, 1.5H); HRMS (ESI-FTICR MS): calcd for  $C_{67}H_{44}N_8O_3RuS^{2+}$  ( $[M^{2+}]$ ): 571.11503; found 571.09923; calcd for  $C_{67}H_{44}F_6N_8O_3PRuS^{2+}$ : 1287.19424  $[M+PF_6]^+$ ; found: 1287.15548.

**Steady-state absorption and emission spectroscopy; emission quantum yields:** UV/Vis absorption spectra were measured on a Varian Cary 5000 instrument in a  $1 \times 1$  cm<sup>2</sup> optical quartz cell with spectroscopic-grade MeCN. Emission spectra were recorded on a Horiba Fluorolog (Jobin Yvon) fluorimeter equipped with double monochromators for excitation and emission. The emission upon 520 nm excitation was detected at  $90^\circ$  with an R928P photomultiplier tube (PMT) detector in single-photon-counting mode with 5.0 nm resolution on the monochromators. The reported spectra were corrected for varying detector sensitivity at different wavelengths. Spectroscopic-grade MeCN purged with Ar(g) to remove oxygen was used. Samples were prepared in  $1 \times 1$  cm<sup>2</sup> optical quartz cells

with an optical density of  $\leq 0.1$  at the excitation wavelength. All samples were Ar(g)-purged for  $> 10$  min additionally prior to measurements, which were performed under Ar(g) pressure. Emission quantum yields were determined from the integrated emission peaks of the corrected spectra, normalized by the optical density at 520 nm.  $[Ru(dqp)]^{2+}$  ( $PF_6^-$ )<sub>2</sub>, in which  $\Phi_{em} = 0.02$ ,<sup>[24]</sup> was measured under the same conditions and used as a reference.

**Time-correlated single-photon counting:** Time-correlated single-photon counting was set up with a regenerative amplified Ti:sapphire system from Coherent, which produced 800 nm pulses of 150 fs duration at 200 kHz repetition rate. The 400 nm pump was obtained by doubling of the Ti:sapphire fundamental. Samples were prepared in air-equilibrated MeCN to an optical density of  $\leq 0.1$  at 400 nm in a  $1 \times 1$  cm<sup>2</sup> quartz optical cell. The sample chamber was optimized for minimal scattering and a combination of a 455 nm cut-off filter and 751 nm bandpass filter was used between the sample and detector to remove scattered pump light and reduce filter emission. A polarizer set to magic angle ( $54.7^\circ$ ) versus the vertically polarized pump was used in front of the detector. The emission was collected perpendicular to the probe on a cooled Hamamatsu R38094-5 microchannel-plate PMT with a response function of  $\sim 80$  ps FWHM. The data contain additional short-lived components, not reported in the text, with no counterpart in the transient absorption measurements, due to filter fluorescence or other experimental defects.

**Nanosecond time-resolved emission and transient absorption spectroscopy:** Time-resolved emission and transient absorption measurements on the nanosecond to microsecond timescale were performed with a frequency-tripled Q-switched Nd:YAG laser (Quantel) pumping an optical parametric oscillator (Opotek) to obtain 520 nm pump light of  $\leq 10$  ns pulse duration. Spectroscopic-grade MeCN purged with Ar(g) to remove oxygen was used. Samples were prepared in  $1 \times 1$  cm<sup>2</sup> optical quartz cells and all samples were Ar(g)-purged for  $> 10$  min additionally prior to measurements, which were performed under Ar(g) pressure. The emission was detected at right angles to the incoming laser beam with a monochromator and an R928-type PMT. The same set-up and detector were used for transient absorption spectroscopy, in which the probe light was provided by a pulsed Xe arc lamp. The output was recorded on a Hewlett–Packard digital oscilloscope and processed with Applied Photophysics LKS60 software.

**Ultrafast transient absorption spectroscopy:** The Ti:sapphire laser system and experimental set-up for transient absorption pump–probe measurements on the femtosecond scale used here have been previously described elsewhere.<sup>[58]</sup> Pump light of 480 nm was obtained by three-wave mixing of the optical paramagnetic amplifier (TOPAS) output at 1440 and 720 nm. Filters were used to remove stray light and obtain a clean pump. The white-light probe was generated from a fraction of the 800 nm Ti:sapphire output passed through an optical delay line ( $< 10$  ns total delay) and focused onto a moving CaF<sub>2</sub> plate. The polarization of the pump was set at magic angle ( $54.7^\circ$ ) relative to that of the probe by using a polarizer and a  $\lambda/2$  plate. Samples were prepared in a  $1 \times 10$  mm<sup>2</sup> optical cell to an approximate optical density of 0.2 at the excitation wavelength in spectroscopic-grade MeCN, purged with Ar(g) prior to sample preparation to remove oxygen. The pump energy at the vertically moving sample cell was reduced by filters to  $< 1 \mu J$  (diameter  $< 400 \mu m$ ) to avoid sample degradation and non-linear effects. The reported spectra are averages of 500–10000 individual measurements. The chirp was much smaller than 5 ps, which is the earliest time at which spectra are shown.

**General considerations and photostability:** The compounds were stored under dark and oxygen-free conditions, and exposed to light and air only for short periods during sample preparation. In general, the solvent was purged with Ar(g) to remove oxygen prior to sample preparation. Steady-state emission and absorption spectroscopy were used in between measurements and scan-to-scan degradation was carefully monitored in the transient absorption measurements.

## Acknowledgements

This work was financially supported by the Swedish Energy Agency, the Knut and Alice Wallenberg Foundation, and the EU/Energy Network project SOLAR-H2 (FP7 contract 212508).

- [1] E. Schrödinger, *What is Life? The Physical Aspects of the Living Cell*, Cambridge University Press, New York, **1944**.
- [2] J. Barber, B. Anderson, *Nature* **1994**, *370*, 31–34.
- [3] B. A. Diner, F. Rappaport, *Annu. Rev. Plant Biol.* **2002**, *53*, 551–580.
- [4] G. Renger in *Comprehensive Series in Photochemistry and Photobiology, Vol. 8* (Eds.: D.-P. Häder, G. Jori), RSC, Cambridge, **2008**.
- [5] J. H. Alstrum-Acevedo, M. K. Brennaman, T. J. Meyer, *Inorg. Chem.* **2005**, *44*, 6802–6827.
- [6] S. Campagna, F. Puntoriero, F. Nastasi, G. Bergamini, V. Balzani, *Top. Curr. Chem.* **2007**, *280*, 117–214.
- [7] J. P. Sauvage, J. P. Collin, J. C. Chambron, S. Guillerez, C. Coudret, V. Balzani, F. Barigelletti, L. De Cola, L. Flamigni, *Chem. Rev.* **1994**, *94*, 993–1019.
- [8] O. S. Wenger, *Coord. Chem. Rev.* **2009**, *253*, 1439–1457.
- [9] M. Falkenström, O. Johansson, L. Hammarström, *Inorg. Chim. Acta* **2007**, *360*, 741–750.
- [10] J.-M. Lehn, M. Kirch, J.-P. Sauvage, *Helv. Chim. Acta* **1979**, *62*, 1345–1384.
- [11] S. Campagna, C. Di Pietro, F. Loiseau, B. Maubert, N. McClenaghan, R. Passalacqua, F. Puntoriero, V. Ricevuto, S. Serroni, *Coord. Chem. Rev.* **2002**, *229*, 67–74.
- [12] F. R. Keene, *Coord. Chem. Rev.* **1997**, *166*, 121–159.
- [13] F. R. Keene, *Chem. Soc. Rev.* **1998**, *27*, 185–193.
- [14] K. A. Opperman, S. L. Mecklenburg, T. J. Meyer, *Inorg. Chem.* **1994**, *33*, 5295–5301.
- [15] M. Borgström, N. Shaikh, O. Johansson, M. F. Anderlund, S. Styring, B. Åkermark, A. Magnuson, L. Hammarström, *J. Am. Chem. Soc.* **2005**, *127*, 17504–17515.
- [16] J. A. Treadway, P. Chen, T. J. Rutherford, F. R. Keene, T. J. Meyer, *J. Phys. Chem. A* **1997**, *101*, 6824–6826.
- [17] T. J. Rutherford, F. R. Keene, *Inorg. Chem.* **1997**, *36*, 2872–2878.
- [18] J.-P. Collin, S. Guillerez, J.-P. Sauvage, F. Barigelletti, L. De Cola, L. Flamigni, V. Balzani, *Inorg. Chem.* **1991**, *30*, 4230–4238.
- [19] P. Lainé, F. Bedioui, E. Amouyal, V. Albin, F. Berruyer-Penaud, *Chem. Eur. J.* **2002**, *8*, 3162–3176.
- [20] O. Johansson, M. Borgström, R. Lomoth, M. Palmblad, J. Bergquist, L. Hammarström, L. Sun, B. Åkermark, *Inorg. Chem.* **2003**, *42*, 2908–2918.
- [21] J. M. Calvert, J. V. Caspar, R. A. Binstead, T. D. Westmoreland, T. J. Meyer, *J. Am. Chem. Soc.* **1982**, *104*, 6620–6627.
- [22] B. J. Coe, D. A. Friesen, D. W. Thompson, T. J. Meyer, *Inorg. Chem.* **1996**, *35*, 4575–4584.
- [23] M. Abrahamsson, M. Jäger, T. Österman, L. Eriksson, P. Persson, H.-C. Becker, O. Johansson, L. Hammarström, *J. Am. Chem. Soc.* **2006**, *128*, 12616–12617.
- [24] M. Abrahamsson, M. Jäger, R. J. Kumar, T. Österman, P. Persson, H.-C. Becker, O. Johansson, L. Hammarström, *J. Am. Chem. Soc.* **2008**, *130*, 15533–15542.
- [25] M. Jäger, L. Eriksson, J. Bergquist, O. Johansson, *J. Org. Chem.* **2007**, *72*, 10227–10230.
- [26] M. Jäger, R. J. Kumar, H. Görls, J. Bergquist, O. Johansson, *Inorg. Chem.* **2009**, *48*, 3228–3238.
- [27] D. Gust, T. A. Moore, A. L. Moore, in *Electron Transfer in Chemistry, Vol. 3* (Ed.: V. Balzani), Wiley-VCH, Weinheim, **2001**, pp. 272–336.
- [28] M. R. Wasielewski, *Chem. Rev.* **1992**, *92*, 435–461.
- [29] A. C. Benniston, G. M. Chapman, A. Harriman, S. A. Roston, *Inorg. Chem.* **2005**, *44*, 4029–4036.
- [30] M. Borgström, O. Johansson, R. Lomoth, H. B. Baudin, S. Wallin, L. Sun, B. Åkermark, L. Hammarström, *Inorg. Chem.* **2003**, *42*, 5173–5184.
- [31] R. A. Berthon, S. B. Colbran, G. M. Moran, *Inorg. Chim. Acta* **1993**, *204*, 3–7.
- [32] K. S. Schanze, K. Sauer, *J. Am. Chem. Soc.* **1988**, *110*, 1180–1186.
- [33] V. Goulle, A. Harriman, J.-M. Lehn, *J. Chem. Soc. Chem. Commun.* **1993**, 1034–1036.
- [34] E. A. Alemán, C. D. Shreiner, C. S. Rajesh, T. Smith, S. A. Garrison, D. A. Modarelli, *Dalton Trans.* **2009**, 6562–6577.
- [35] B. I. Greene, R. M. Hochstrasser, R. B. Weisman, *J. Chem. Phys.* **1979**, *70*, 1247–1259.
- [36] E. Laviron, *J. Electroanal. Chem.* **1986**, *208*, 357–372.
- [37] P. Wardman, *J. Phys. Chem. Ref. Data* **1989**, *18*, 1637–1657.
- [38] J. A. Schmidt, A. Siemiarczuk, A. C. Weedon, J. R. Bolton, *J. Am. Chem. Soc.* **1985**, *107*, 6112–6114.
- [39] J. A. Schmidt, A. R. McIntosh, A. C. Weedon, J. R. Bolton, J. S. Connolly, J. K. Hurley, M. R. Wasielewski, *J. Am. Chem. Soc.* **1988**, *110*, 1733–1740.
- [40] The amount of excited state subtracted from the product spectrum (at 5 ns) was scaled by the amplitude ( $\Delta O.D.$ ) at 427 and 430 nm for **1a** and **3a**, respectively. The reference dyads **2a** and **4a** show isosbestic points at these wavelengths, and thus the only contribution to the spectrum at these wavelengths should be that of the product state. The percentage of subtracted excited-state spectrum is 5% in **1a** and 40% in **3a**, in good agreement with the fraction of hydroquinone found in steady-state emission quantum yield measurements and NMR data.
- [41] S. A. Alkaitis, G. Beck, M. Grätzel, *J. Am. Chem. Soc.* **1975**, *97*, 5723–5729.
- [42] J. R. Darwent, K. Kalyanasundaram, *J. Chem. Soc. Faraday Trans. 2* **1981**, *77*, 373–382.
- [43] P. S. Rao, E. Hayon, *J. Phys. Chem.* **1973**, *77*, 2274–2276.
- [44] K. B. Patel, R. L. Willson, *J. Chem. Soc. Faraday Trans. 1* **1973**, *69*, 814–825.
- [45] Calculated as  $-(\Delta G_{ET}) = E_{00} + e[E_{1/2}(Q^{0-}) - E_{1/2}(Ru^{3+2+})]$  and  $-(\Delta G_{ET}) = E_{00} + e[E_{1/2}(Q^{-0}) - E_{1/2}(PTZ^{+0})]$ , respectively. The Coulombic work term is assumed to be negligible.
- [46] Calculated as  $-(\Delta G_{ET}) = E_{00} + e[E_{1/2}(RuL_2^{2+/+}) - E_{1/2}(PTZ^{+0})]$ .
- [47] E. Danielson, C. M. Elliott, J. W. Merkert, T. J. Meyer, *J. Am. Chem. Soc.* **1987**, *109*, 2519–2520.
- [48] D. R. Striplin, S. Y. Reece, D. G. McCafferty, C. G. Wall, D. A. Friesen, B. W. Erickson, T. J. Meyer, *J. Am. Chem. Soc.* **2004**, *126*, 5282–5291.
- [49] J. M. Weber, M. T. Rawls, V. J. MacKenzie, B. R. Limoges, C. M. Elliott, *J. Am. Chem. Soc.* **2007**, *129*, 313–320.
- [50] K. A. Maxwell, M. Sykora, J. M. DeSimone, T. J. Meyer, *Inorg. Chem.* **2000**, *39*, 71–75.
- [51] S. L. Mecklenburg, D. G. McCafferty, J. R. Schoonover, B. M. Peek, B. W. Erickson, T. J. Meyer, *Inorg. Chem.* **1994**, *33*, 2974–2983.
- [52] L. F. Cooley, S. L. Larson, C. M. Elliott, D. F. Kelley, *J. Phys. Chem.* **1991**, *95*, 10694–10700.
- [53] E. Baranoff, J.-P. Collin, L. Flamigni, J.-P. Sauvage, *Chem. Soc. Rev.* **2004**, *33*, 147–155.
- [54] Determined relative to  $[Ru(bpy)_3]^{2+}$  upon 480 nm excitation, by using  $\Delta\epsilon_{450}[Ru^{II}(bpy)_3^*] \leq -1.0 \times 10^4 \text{ M}^{-1} \text{ cm}^{-1}$  (from A. Yoshimura, M. Z. Hoffman, H. Sun, *J. Photochem. Photobiol. A* **1993**, *70*, 29–33).
- [55] G. E. Adams, B. D. Michael, *J. Chem. Soc. Faraday Trans.* **1967**, *1171*–1180.
- [56] The non-active hydroquinone fraction of 5% in **1a** and 40% in **3a** has been taken into account when evaluating the maximum ground-state bleach.
- [57] J. Elhaik, C. M. Pask, C. A. Kilner, M. A. Halcrow, *Tetrahedron* **2006**, *62*, 291–298.
- [58] S. Karlsson, J. Modin, H.-C. Becker, L. Hammarström, H. Grennberg, *Inorg. Chem.* **2008**, *47*, 7286–7294.

Received: October 2, 2009  
Published online: January 19, 2010